Bioorganic Chemistry 90 (2019) 102844

Contents lists available at ScienceDirect

Bioorganic Chemistry

journal homepage: www.elsevier.com/locate/bioorg

Synthesis, modeling and biological evaluation of some pyrazolo[3,4-d] pyrimidinones and pyrazolo[4,3-e][1,2,4]triazolo[4,3-a]pyrimidinones as anti-inflammatory agents

Gina N. Tageldin[a,*], Tamer M. Ibrahim[b,*], Salwa M. Fahmy[a], Hayam M. Ashour[a], Mounir A. Khalil[a], Rasha A. Nassra[c], Ibrahim M. Labouta[a]

[a] Department of Pharmaceutical Chemistry, Faculty of Pharmacy, Alexandria University, Alexandria 21521, Egypt
[b] Pharmaceutical Chemistry Department, Faculty of Pharmacy, Kafrelsheikh University, Kafr El-Sheikh 33516, Egypt
[c] Department of Medical Biochemistry, Faculty of Medicine, Alexandria University, Alexandria, Egypt

ARTICLE INFO

Keywords:
Pyrazolo[3,4-d]pyrimidinones
Pyrazolo[4,3-e][1,2,4]triazolo[4,3-a] pyrimidinones
Anti-inflammatory activity
Ulcerogenic effect
COX-1/COX-2 selectivity index
Docking experiments

ABSTRACT

New pyrazolo[3,4-*d*]pyrimidinone and pyrazolo[4,3-e][1,2,4]triazolo[4,3-*a*]pyrimidinone derivatives were synthesized. They have been evaluated for their anti-inflammatory activity using in vitro (COX-1/COX-2) inhibitory assay. Moreover, compounds with promising in vitro activity and COX-1/COX-2 selectivity indices were subjected for *in vivo* anti-inflammatory testing using formalin induced paw edema and cotton-pellet induced granuloma assays for acute and chronic models, respectively. Compounds (2c, 3i, 6a, 8 and 12) showed promising COX-2 inhibitory activity and high selectivity compared to celecoxib. Most of the compounds exhibited potential anti-inflammatory activity for both in vivo acute and chronic models. Almost all compounds displayed safe gastrointestinal profile and low ulcerogenic potential guided by histopathological examination. Furthermore, molecular docking experiments rationalized the observed i***n vitro anti-inflammatory activity of*** selected candidates. In silico predictions of the pharmacokinetic and drug-likeness properties recommended accepted profiles of the majority of compounds. In conclusion, this work provides an extension of the chemical space of pyrazolopyrimidinone and pyrazolotriazolopyrimidinone chemotypes for the anti-inflammatory activity.

1. Introduction

Non-steroidal anti-inflammatory drugs (NSAIDs) are widely recommended agents in inflammatory diseases [1]. The pharmacological activity of NSAIDs is correlated to their ability to inhibit cyclooxygenase enzyme (COX) isoforms; COX-1 and COX-2 which catalyzes the bioconversion of arachidonic acid (AA) to inflammatory prostaglandins (PGs). PGs mediate a number of characteristic features of the body's response to tissue injury or inflammation [2,3]. However, prolonged clinical indication of NSAIDs is connected to several adverse effects including gastrointestinal (GI) ulcers, hemorrhage, and nephrotoxicity that resulted from non-specific inhibition of COXs [3–5]. Accordingly, selective COX-2 inhibitors such as celecoxib were developed (**I,** Fig. 1) that should maintain the medical efficiency of classical NSAIDs with reduced GI side effects [6]. However, associated cardiovascular adverse effects led to reconsideration of their clinical use [7]. Therefore, development of novel compounds possessing both desired therapeutic activity and improved selectivity is still a demand.

Pyrazolo[3,4-*d*]pyrimidinone scaffold were involved in a wide variety of pharmacologically active compounds including anti-inflammatory drugs [8–14]. For example, DPP; (N^4-benzyl-1-(*tert*-butyl)-N^6,N^6-dimethyl-1*H*-pyrazolo[3,4-*d*]pyrimidinone-4,6-diamine) (**II,** Fig. 1) possessed both anti-inflammatory and analgesic activities [15,16]. In addition, it showed greater selectivity to COX-2 enzyme by 66 fold [17]. Interestingly, the anti-inflammatory activity of some pyrazolo[3,4-*d*]pyrimidinones were resulted from dual inhibition to COXs and inducible nitric oxide synthase (iNOS) enzymes [18]. For instance, compound (**III,** Fig. 1) exhibited high potency and COX-2 selectivity compared to indomethacin [18].

On the other hand, the 1,2,4-triazole scaffold was reported to be incorporated in several anti-inflammatory drug candidates [19–27]. Moreover, some reports claimed the positive impact of fusing the 1,2,4-triazole ring with pyrazolo[3,4-*d*]pyrimidinone skeleton on the anti-inflammatory and analgesic activities (**IVa, IVb, V,** Fig. 1) [28–30].

* Corresponding authors.
E-mail addresses: gina.tageldin@alexu.edu.eg (G.N. Tageldin), Tamer_Mohamad@pharm.kfs.edu.eg (T.M. Ibrahim).

https://doi.org/10.1016/j.bioorg.2019.03.018
Received 30 December 2018; Received in revised form 3 March 2019; Accepted 9 March 2019
Available online 12 March 2019
0045-2068/

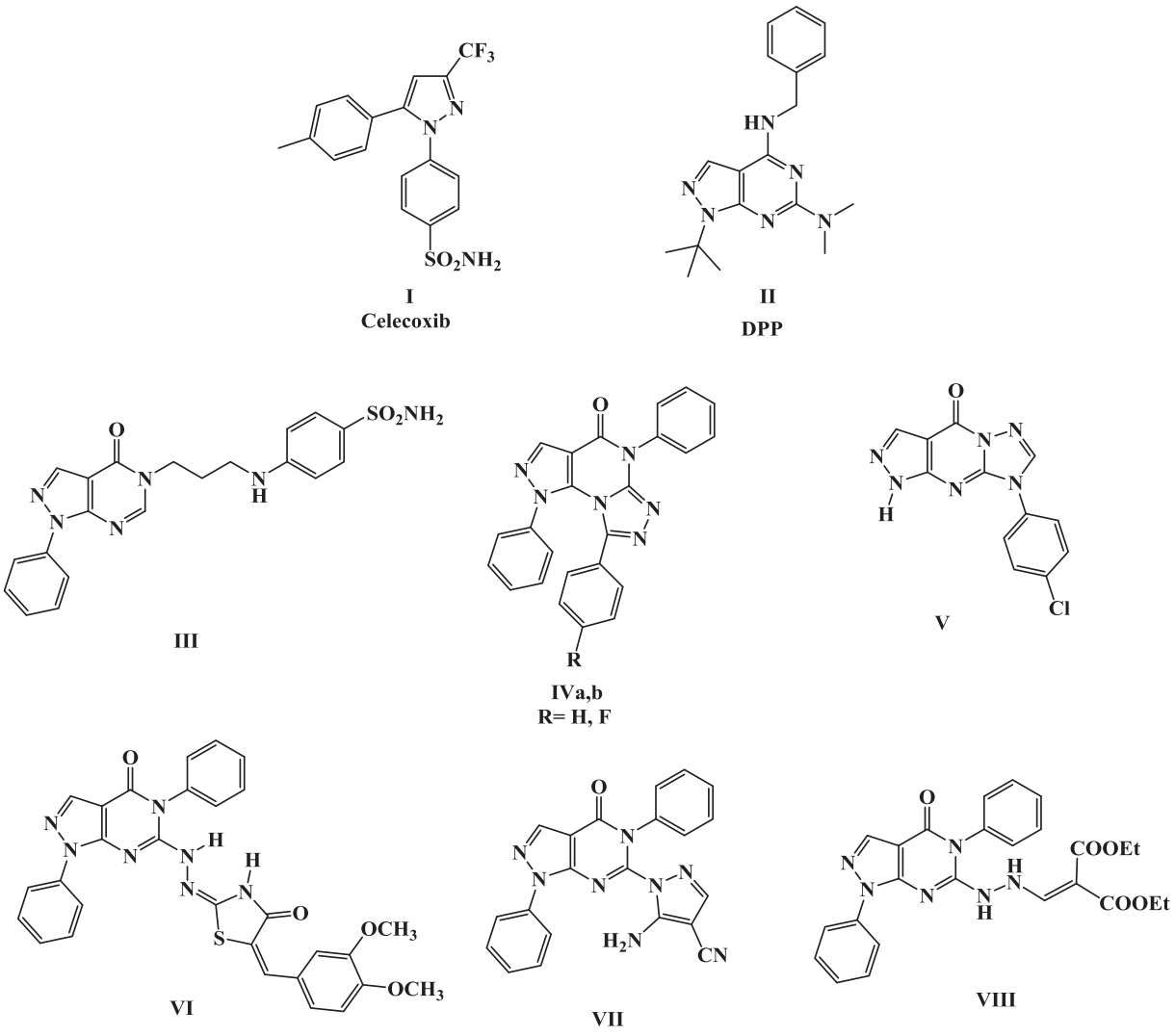

Fig. 1. Chemical structures of compounds I-VIII.

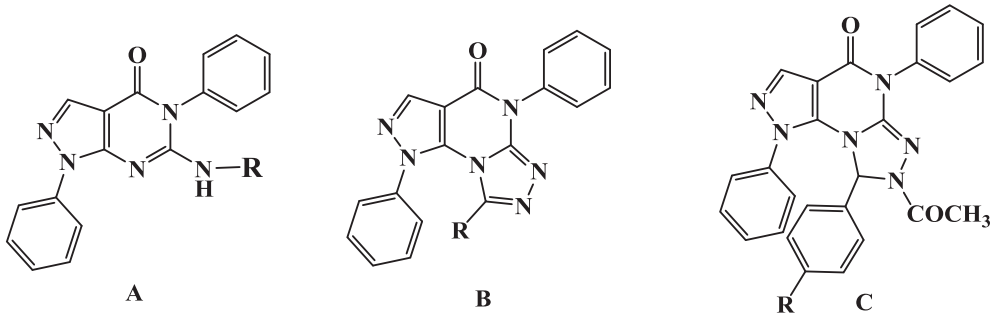

Fig. 2. Design of new pyrazolo[3,4-*d*]pyrimidinones and pyrazolo[4,3-e][1,2,4]triazolo[4,3-*a*]pyrimidinones as COX-2 inhibitors.

In the course of a research program related to exploring new active structures devoid of the unfavorable side effects associated with classical NSAIDs, we have previously reported the synthesis and anti-inflammatory activity of some pyrazolo[3,4-*d*]pyrimidinones substituted with vast numbers of functional groups and attached to various heterocyclic ring systems through different linkages [8,9]. Particularly, romising anti-inflammatory activity and remarkable gastrointestinal safety were exhibited by these structures **VI** [8], **VII** [9] and **VIII** [9] (Fig. 1). Invigorated by these results, we planned to enrich the chemical space of the promising pyrazolo[3,4-*d*]pyrimidinones chemotypes for anti-inflammatory activity [31]. For this, we linked the pyrazolo[3,4-*d*] pyrimidinone nucleus to various substituents at position 6 (**Structure A,** Fig. 2). The selected substituents were chosen to afford different electronic, lipophilic and steric environment to the structures that could affect the biological activity towards the target. Moreover, it was interesting to extend the biological exploration of the pyrazolo[3,4-*d*] pyrimidinone skeleton by annulation with triazole ring system. Such annulation was supposed to maximize interaction with hydrophobic residues in the active site of COX-2 enzyme. In addition, this would improve selectivity since the designed fused pyrazolopyrimidinone derivatives (**Structures B** and **C,** Fig. 2) will be relatively large to accommodate specific binding event within the smaller COX-1 active site.

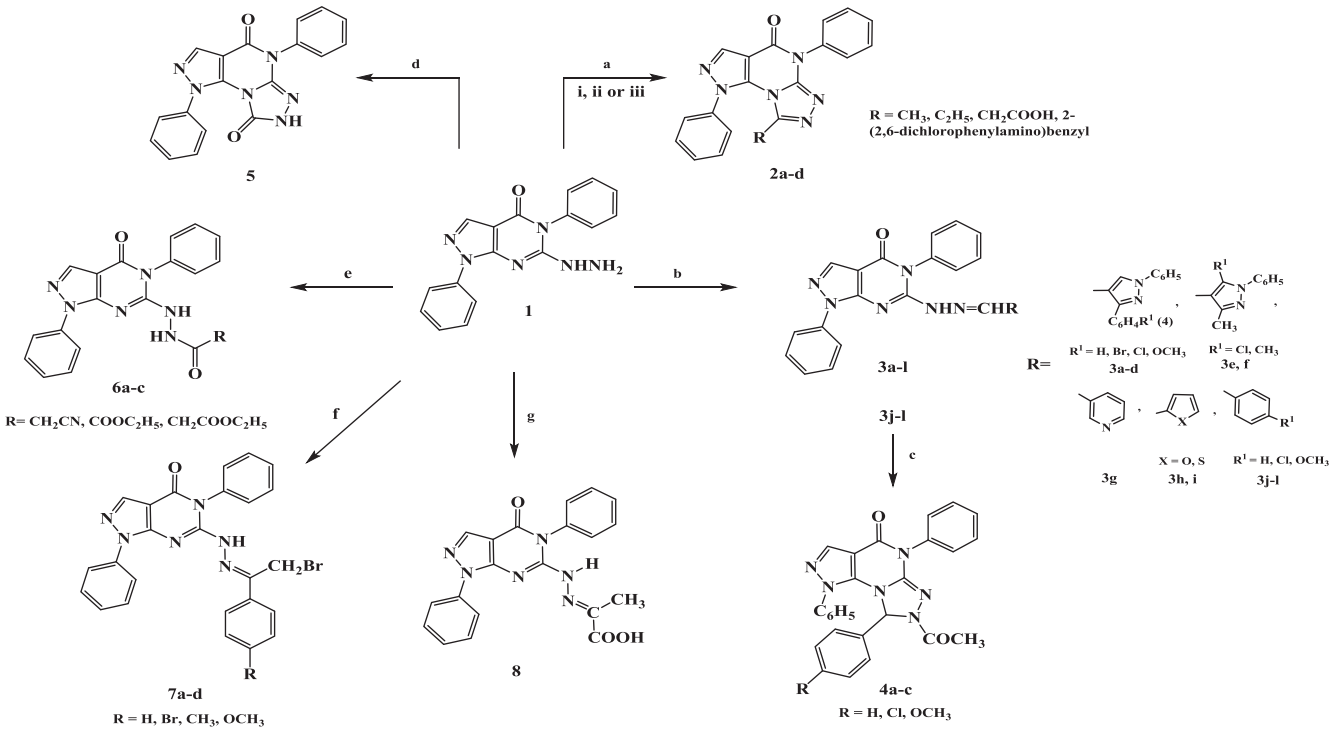

Scheme 1. Reagents and conditions: (a) appropriate acid; (i) reflux, 3 h; (ii) TSA, fusion at 200 °C, 1 h; (iii) CH_2Cl_2/DCC, rt, 24 h; (b) appropriate aldehyde, abs. EtOH, reflux, 2 h; (c) Ac_2O, reflux, 8 h; (d) excess urea, fusion at 200 °C, 2 h; (e) appropriate ester, reflux, 15 min to 4 h; (f) 4-substituted phenacyl bromide, abs. EtOH, reflux, 12 h or dioxane/ piperidine, reflux, 4 h; (g) Na pyruvate, EtOH/ gl. AcOH, reflux, 4 h.

For evaluating the designed compounds, we conducted in *vitro* COX-1/COX-2 inhibition assay and *in vivo* anti-inflammatory activity in two inflammatory models (acute and chronic). This would construct structure-activity correlation based on different modifications. To evaluate the ulcerogenic potential of the designed compounds, we carried out histopathological examination on the gastric layers of tested rats' stomachs. Furthermore, we conducted molecular docking experiments to rationalize the observed *in vitro* anti-inflammatory activity of some selected candidates. Also, in silico predictions of the pharmacokinetic and drug-likeness properties were performed for selected compounds.

2. Results and discussion

2.1. Chemistry

The synthetic strategies adopted for the synthesis of the target compounds are depicted in Schemes 1 and 2. In Scheme 1, cyclization of the hydrazine derivative (1) [32] with excess amount of glacial acetic acid and propanoic acid afforded the corresponding pyrazolo-triazolopyrimidinones (2a) [29] and (2b), respectively. Whereas, the acetic acid derivative **(2c)** was obtained by fusion of **(1)** with malonic acid in the presence of p-toulenesulphonic acid. On the other hand, stirring **(1)** with diclofenac acid [33,34] in methylene chloride using N,N′-dicyclohexylcarbodiimide (DCC) at room temperature afforded **(2d)**. **^{1}H NMR spectra** of compounds **(2a-d)** showed a singlet at 2.45 ppm due to CH_3 protons in **(2a)**, triplet at 0.91 ppm and quartet at 1.80 ppm assigned for CH_2CH_3 protons in **(2b)** and a singlet at 2.48 ppm attributed to CH_2 protons in **(2c)**, however, compound **(2d)** showed a singlet at 3.22 ppm assigned for CH_2 protons. It is worth-mentioning that compound **(2a)** was reported to be prepared in a lower yield via heating the hydrazine **(1)** with triethyl orthoacetate [29]. Hydrazones **(3a-l)** were prepared by condensation of the hydrazine **(1)** with different aldehydes (pyrazole aldehydes [35–37], heterocyclic aldehydes or aromatic aldehydes) in absolute ethanol. **^{1}H NMR spectra** of compounds **(3c,e,f,g)** showed a D_2O-exchangeable singlets at

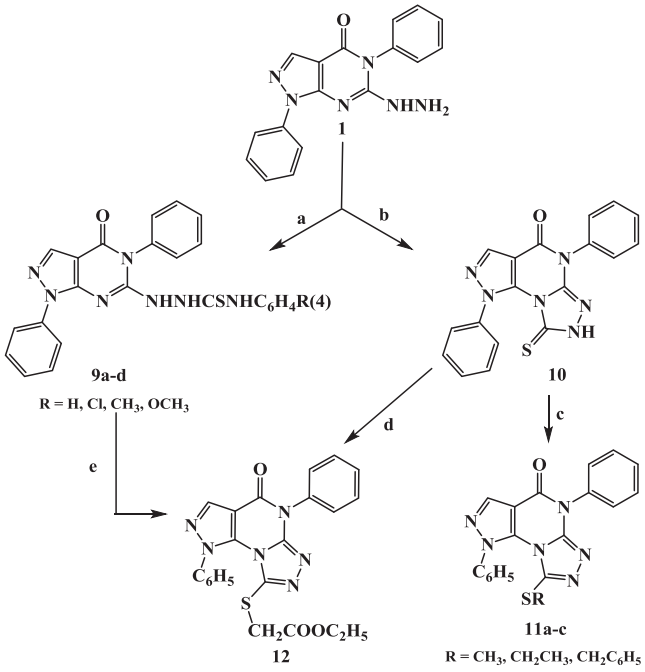

Scheme2. Reagents and conditions: (a) appropriate aryl isothiocyanate, CH_2Cl_2, rt, 24 h; (b) phenyl isothiocyanate, dry dioxane, reflux, 14 h; (c) appropriate alkyl or aryl halide, dry DMF, anhydrous K_2CO_3, rt, 24 h; (d) $BrCH_2COOC_2H_5$, dry DMF, anhydrous K_2CO_3, rt, 24 h; (e) $BrCH_2COOC_2H_5$, abs. EtOH, reflux, 8 h.

9.45–10.20 ppm assigned for NH, in addition to a singlet at 8.14–8.21 ppm assigned for N=CH proton. In the present study, the target acetylated triazole derivatives **(4a-c)** were prepared by heating hydrazones **(3j-l)** in excess acetic anhydride. **^{1}H NMR spectra** of compounds **(4a-c)** showed signals assigned for acetyl CH_3 protons at

their expected chemical shifts, in addition to signals at 6.83–6.89 ppm assigned for pyrazolotriazolopyrimidinone C_8 protons. **^{13}C NMR spectrum** of compound **(4a)** revealed signals due to CH_3, pyrazolotriazolopyrimidinone C_8 and acetyl C═O at their expected chemical shifts. Moreover, the triazolo derivative **(5)** was eventually obtained by fusion **(1)** with excess urea at 200 °C. The **IR spectrum** of compound **(5)** characterized by strong absorption bands at 3201 and 1760 cm^{-1} corresponding to NH and the C═O functions, respectively, while, its **^{1}H NMR spectrum** revealed a D_2O-exchangeable singlet at 13.00 ppm assigned to NH proton. Reflux the hydrazine precursor **(1)** with various esters (ethyl cyanoacetate, diethyl oxalate and diethyl malonate) yielded the corresponding hydrazides **(6a-c)**. **IR spectra** of compounds **(6a-c)** were characterized by absorption bands at 3411–3410, 3251–3241 cm^{-1}corresponding to NH function, absorption band at 2258 cm^{-1} attributed to CN in **(6a)**, in addition to a stretching absorption band at 1756–1740 cm^{-1} due to ester C═O function in compounds **(6b,c)**. **^{1}H NMR spectra** for compounds **(6b,c)** revealed protons for the ester group at their expected chemical shifts. Heating **(1)** with phenacyl bromides in boiling ethanol or dioxane containing catalytic amount of piperidine gave arise to the hydrazones **(7a-d)**. **^{1}H NMR spectra** of compounds **(7b,d)** showed duplication of all signals indicating presence of E and Z isomers; for example they revealed two D_2O-exchangeable singlets at 10.05, 10.15 ppm and 9.95, 10.09 ppm respectively assigned for two NH protons (E and Z isomers). Singlets at 3.72, 3.80 and 3.90, 3.96 ppm assigned for CH_2 protons (E and Z isomers). In addition, two singlets at 3.80 and 3.82 ppm due to methoxy protons (E and Z isomers) in compound **(7d)** were also observed. On the other hand, heating **(1)** with sodium pyruvate in ethanol/glacial acetic acid mixture yielded the hydrazone derivative **(8)**.

In Scheme 2**,** boiling the hydrazine precursor **(1)** with phenyl isothiocyanate in dioxane did not afford the corresponding thiosemicarbazide **(9a)**, the 8-thioxo pyrazolotriazolopyrimidinone **(10)** was separated instead. The mechanism of formation of **(10)** could be explained by cyclodeamination of the resulted thiosemicarbazide intermediate (Supplementary Material (SM), Fig. S1). Literature survey revealed that compound **(10)** was previously prepared using carbon disulfide in methanolic potassium hydroxide [29]. The chemical structure of compound **(10)** was verified by analytical and spectral data. Fortunately, the desired thiosemicarbazide derivatives **(9a-d)** were successfully prepared by stirring **(1)** with aryl isothiocyanates in methylene chloride at room temperature. **^{1}H NMR spectra** of compounds **(9a,c)** showed three D_2O-exchangeable singlets at 8.74, 9.45, 9.65 and 8.75, 9.46, 9.62 ppm assigned for three NH protons, respectively. Stirring the thioxo derivative **(10)** with the appropriate alkyl or aryl halides gave arise to the corresponding S-alkylated derivatives **(11a-c)**. **^{1}H NMR spectra** of compounds **(11a,b)** showed a singlet for SCH_3 in **(11a)**, triplet and quartet due to SCH_2CH_3 protons in **(11b)** at their expected chemical shifts. Also, **^{13}C NMR spectrum** for **(11b)** showed signals for CH_3 and SCH_2 carbons at 14.00 and 29.40 ppm, respectively. The S-alkylated derivative **(12)** was prepared by stirring the thioxo derivative **(10)** with ethyl bromoacetate in dry dimethylformamide (DMF) at room temperature **(Method A)** or by heating thiosemicarbazides **(9a-d)** with ethyl bromoacetate in the presence or absence of a base **(Method B)**. The possible mechanism for cyclodeamination and formation of the sulfanyl acetate ester **(12)** is illustrated in (SM, Fig. S2). **IR spectrum** of the latter revealed strong stretching absorption band at 1734 cm^{-1} due to ester C═O function and its **^{1}H NMR spectrum** displayed the triplet and quartet of the ester group at their expected chemical shifts and a singlet at 4.27 ppm integrated for the CH_2CO protons. Further confirmation of the structure was derived from its **^{13}C NMR spectrum** that showed signals at 14.52, 39.66 and 62.28 ppm corresponding to CH_3 and SCH_2 and OCH_2 carbons, respectively, in addition to a signal at 167.98 ppm attributed to ester C═O.

Table 1
In vitro COX-1 and COX-2 enzymes inhibitory activities, IC_{50} values and selectivity indices (SI) of the tested compounds:

Comp. No.	IC_{50} (μM)[a] COX-1	IC_{50} (μM) COX-2	SI[b] (COX-1/COX-2)
2a	7.24	2.04	3.50
2b	5.55	1.38	4.02
2c	4.33	0.58	7.46
2d	7.42	1.28	5.79
3a	4.52	1.04	4.30
3b	7.33	1.89	3.87
3c	8.54	2.56	3.30
3d	5.91	1.49	3.96
3e	2.41	0.47	5.13
3f	6.74	1.34	5.02
3g	6.56	1.24	5.29
3h	9.24	2.94	3.14
3i	3.98	0.63	6.30
4a	5.24	0.93	5.63
4b	8.71	2.32	3.75
4c	6.23	1.54	4.06
4d	5.29	0.99	5.34
5	4.36	1.11	3.93
6a	4.65	0.38	12.23
6b	6.52	1.45	4.49
6c	5.29	0.99	5.34
8	5.87	0.74	7.93
11b	6.45	1.63	3.90
11c	8.56	1.97	4.34
12	2.85	0.29	9.82
Celecoxib	5.46	0.78	7.23
Diclofenac Sodium	6.74	1.10	6.12

[a] Values are means of three determinations acquired using an ovine COX-1/COX-2 assay kit (catalog no. 760111, Cayman Chemicals, MI, USA) and the deviation from the mean is ± 10% of the mean value
[b] *In vitro* COX-2 selectivity index (COX-1 IC_{50}/COX-2 IC_{50})

2.2. Biological evaluation

2.2.1. In vitro cyclooxygenase (COX) inhibition assay

All the synthesized compounds were tested for their *in vitro* inhibition of COX-1 and COX-2 isoenzymes using Cayman colorimetric COX (ovine) inhibitor screening assay kit. The Colorimetric COX Inhibitor Screening Assay utilizes the peroxidase component of cyclooxygenase. The peroxidase activity was assayed colorimetrically by monitoring the appearance of oxidized *N,N,N′,N′*-tetramethyl-1,4-phenylenediamine (TMPD) which is produced during the reduction of PGG2 to PGH2, at 590 nm. The concentration produced 50% inhibition of COX-1 and COX-2 isoenzymes (IC_{50} values) and the selectivity indices (SI = IC_{50} COX-1/ IC_{50} COX-2) of the test compounds were determined and results are recorded in Table 1.

In general, all the tested compounds showed relatively higher selectivity towards COX-2 than COX-1. Compounds (**2b, 2c, 3a, 3d, 3e, 3g, 3i, 4a, 4c, 5, 6a, 6b, 6c, 8, 11b** and **12)** showed IC_{50} values towards COX-1 (IC_{50} = 2.41–5.55 μM) lower than celecoxib and diclofenac sodium (IC_{50} = 5.64 and 6.74 μM, respectively). On the other hand, compounds (**2c, 3e, 3i, 6a, 8,** and **12**) exhibited high COX-2 inhibitory activity (IC_{50} = 0.29–0.74 μM) which was lower than celecoxib (IC_{50} = 0.78 μM). Further investigation of the *in vitro* results revealed that compounds (**2c, 6a, 8** and **12)** possessed selectivity indices (SI = 7.93–12.23) higher than both references diclofenac sodium (SI = 6.12) and celecoxib (SI = 7.23). Among these compounds, compound **(6a)** emerged with selectivity index (SI = 12.23) nearly double that of diclofenac sodium and celecoxib. On the other hand, compound (3i) showed selectivity index (SI = 6.30) higher than diclofenac sodium and nearly equivalent to celecoxib.

Based on the *in vitro* results compounds showing selectivity indices higher or nearly equivalent to the reference drugs were selected for further evaluation of their *in vivo* anti-inflammatory activities.

Table 2
In vivo anti-inflammatory activities of selected compounds in formalin-induced rat paw edema bioassay (acute inflammation model).

Comp. No.	Volume of edema (cm^3) Mean ± SD		% Inhibition (% AI)
	0	4 h	
2c	0.5 ± 0.1	0.6[a] ± 0.1	78.6
2d	0.5 ± 0.0	0.5[a] ± 0.1	78.6[b]
3e	0.5 ± 0.0	0.6[a] ± 0.0	64.3
3g	0.5 ± 0.0	0.6[a] ± 0.0	50.0
3i	0.5 ± 0.0	0.6[a] ± 0.1	78.6[b]
4a	0.5 ± 0.0	0.7 ± 0.0	21.4[b]
6a	0.5 ± 0.0	0.6[a] ± 0.1	71.4
8	0.5 ± 0.0	0.6[a] ± 0.0	64.3
12	0.5 ± 0.0	0.6[a] ± 0.1	71.4
Celecoxib	0.5 ± 0.0	0.6 ± 0.1	46.4
Diclofenac Sodium	0.5 ± 0.0	0.6[a] ± 0.0	50.0
Control	0.5[b] ± 0.0	0.7 ± 0.1	–

[a] Statistically significant difference in comparison with control group.
[b] Statistically significant difference in comparison with diclofenac sodium treated group.

2.2.2. In vivo anti-inflammatory activity

2.2.2.1. Formalin-induced paw edema bioassay. In this acute inflammatory model, each test compound **(2c, 2d, 3e, 3g, 3i, 4a, 6a, 8** and **12)** was dosed orally at dose of (5 mg/kg body weight) for seven days prior to induction of inflammation by formalin injection. [38,39] Celecoxib and diclofenac sodium were utilized as reference drugs at a dose of (5 mg/kg, po). The anti-inflammatory activity was then calculated 4 h after induction of inflammation and presented in Table 2 as the mean paw volume (cm^3) ± SD and the percentage anti-inflammatory activity (AI %).

A comparative study of the anti-inflammatory activity of the test compounds relative to the reference drugs indicated that the tested compounds except for (3g and 4a) showed anti-inflammatory activity (% AI = 64.3–78.6) superior to both diclofenac sodium and celecoxib.

2.2.2.2. Cotton pellet-induced granuloma assay. In order to investigate the test compounds' efficacy against the later proliferative phase of inflammation caused by tissue degeneration and fibrosis, the cotton pellet induced granuloma assay was applied [40]. The results listed in Table 3 represent the mean changes in weight of dry cotton in (mg) ± SD in animals pretreated with the reference drugs and test compounds **(2c, 2d, 3e, 3g, 3i, 4a, 6a, 8** and **12)** after 7 days from the insertion of the cotton pellet and induction of inflammation, together with the percent inhibition of granuloma by the test compounds (% anti-inflammatory activity).

Table 3
In vivo anti-inflammatory activities of selected compounds in Cotton pellet induced granuloma test (Chronic inflammation model).

Comp. No.	Dry weight of granuloma (mg)	% Granuloma inhibition
2c	26.3[a]	43.4
2d	34.2[b]	26.5
3e	45.9	1.4
3g	44.7	3.9
3i	41.7	10.3
4a	42.8	8.0
6a	24.7[ab]	46.9
8	32.8[a]	29.5
12	35.8[a]	23.2
Celecoxib	50.5	8.6
Diclofenac Sodium	29.7[a]	36.1
Control	46.5	–

[a] Statistically significant difference in comparison with control group.
[b] Statistically significant difference in comparison with celecoxib treated group.

The results revealed that compounds **(2c** and **6a)** exhibited anti-inflammatory effect (% inhibition of granuloma = 43.4 and 46.9, respectively) superior to both celecoxib and diclofenac sodium (% inhibition of granuloma = 8.6 and 36.1, respectively). On the other hand, compounds **(2d, 8** and **12)** displayed anti-inflammatory activity (% inhibition of granuloma = 23.2–29.5) higher than celecoxib. However, compounds **(3e, 3g** and **4a)** were less active than both references.

2.2.3. Structure-activity relationship (SARs)

A deep insight in the structures of the newly synthesized compounds revealed that they represent two different classes of compounds; pyrazolo[3,4-*d*]pyrimidinones and pyrazolo[4,3-e][1,2,4]triazolo[4,3-*a*] pyrimidinones. Regarding the pyrazolo[3,4-*d*]pyrimidinones; the hydrazones **(3e, 3g, 3i, 8)** and the cyano acetohydrazide derivative **(6a)** showed remarkable anti-inflammatory activity in the acute model that was superior or equivalent to the reference drugs; nevertheless they showed weak activity in the chronic model except for **(6a)** which was superior to both references. Concerning the pyrazolotriazolopyrimidinones, compounds comprising CH_2COOH **(2c),** SCH_2COOEt **(12),** or 2-(2,6-dichlorophenylamino)benzyl **(2d)** moieties on the triazole ring showed anti-inflammatory activity higher than diclofenac sodium in the acute model, however, they showed weak activity in the chronic model except for compound **(2c)** that was superior to both diclofenac sodium and celecoxib. Introduction of phenyl moiety to triazole ring as in case of **(4a)** reduced the anti-inflammatory activity in both models. Interestingly, compound **(2c** and **2d)** showed same activity in the acute model which was superior to diclofenac sodium. However, in the chronic model only compound **(2c)** showed anti-inflammatory activity superior to diclofenac sodium while **(2d)** displayed lower activity compared to the reference.

A collective interpretation of the anti-inflammatory activity of the test compounds in pre-mentioned screens (Tables 2 and 3) revealed that the pyrazolotriazolopyrimidinone derivative **(2c)** and the pyrazolopyrimidinone derivative **(6a)** showed pronounced anti-inflammatory activity in both inflammatory models suggesting that such compound might be effective in controlling both acute and chronic inflammation.

2.2.4. Gastric ulcerogenic activity:

The tested compounds that exhibited *in vitro* selectivity indices higher or nearly equivalent to reference drugs towards COX-2 enzyme were further evaluated for their ulcerogenic potential in rats [41,42]. Gross observation of the isolated rats' stomachs showed a normal stomach texture for the tested compounds **(2d, 3e, 3g, 3i, 4a, 6a, 8** and **12)** as well as the reference celecoxib. While for compound **(2c)** variable degrees of hyperemia was observed (SM, Fig. S3). Further histopathological examination was performed to confirm the degree of inflammatory reaction in the gastric layers of the treated rats' stomachs. Histopathological examination revealed that compounds **(2d, 3e, 3g, 3i, 4a, 6a, 8** and **12)** showed superior gastrointestinal safety profile (free, normal gastric and esophageal mucosa) as well as celecoxib and diclofenac sodium (SM, Fig. S4a). While, the mucosal surface in case of compound **(2c)** showed beside gastro-esophageal inflammation, few lymphocytic collections. (SM, Fig. S4b).

2.3. Molecular modeling

2.3.1. Molecular docking

The aim of this section is to rationalize the observed *in vitro* biological activity towards COX-2 enzyme. We selected the most active compounds **2c**, **3i**, **6a**, **8** and **12** for docking experiments since they possess the highest selectivity indices for COX-1/COX-2 inhibition and represent the two different pyrazolo[3,4-*d*]pyrimidinone and pyrazolo [4,3-e][1,2,4]triazolo[4,3-*a*]pyrimidinone chemotypes.

Based on a previous *in silico* study to select a COX-2 model[26], we used the human COX-2 crystal structure (PDB: 5IKQ) for the docking

Table 4
Comparison of the docking performance of **2c**, **3i**, **6a**, **8** and **12** against COX-2 and COX-1 enzymes.

Compound	Docking Fitness	
	COX-2	COX-1
2c	59.99	Non-specific binding[b]
3i	61.85	Non-specific binding
6a	49.03	Non-specific binding
8	49.99	Non-specific binding
12	68.12	Non-specific binding
Celecoxib[a]	81.95	53.62

[a] Docking results of celecoxib and indomethacin are freely adapted from our previous study [26,49]. The docking score is expressed as fitness of ChemPLP scoring function of GOLD (v 5.2).[50–53].
[b] Non-specific binding indicates interactions with residues outside the binding site.

experiments.

Elucidating the observed *in vitro* selectivity of **2c**, **3i**, **6a**, **8** and **12** towards COX-2 over COX-1 by docking experiments, we find that these compounds are not able demonstrate a specific binding event in COX-1 binding site (Table 4). This observation is augmented by the fact that the volume of the binding site of COX-1 is much smaller than COX-2 [43–45]. Besides, the size features (e.g., molecular weight) of **2c**, **3i**, **6a**, **8** and **12** are generally greater than the average range of the diverse and representative COX-1 and COX-2 ligands of DEKOIS 2.0 benchmark sets [26,46-48].

Describing the best docked poses of the selected compounds in the binding site of COX-2 showed favorable types interactions in the key catalytic residues. For instance, the docking pose of **2c** shows H-bonding interactions with the side chains of Tyr385 with its acetate moiety, as shown in Fig. 3. The 1-phenyl substituent attached on the core pyrazolo[4,3-e][1,2,4]triazolo[4,3-*a*]pyrimidin appeared to demonstrate hydrophobic interaction with the hydrophobic side chains of Trp387, Met522 and Phe518 from one perspective. The other 5-phenyl substituent is packed between the side chains of Leu359 and Val116 and Leu531, whereas, π-arene interaction between Ala527 and the core pyrazolo[4,3-e][1,2,4]triazolo[4,3-*a*]pyrimidin can be observed.

The postulated binding pose of **3i** demonstrated mainly hydrophobic interactions with the binding site residues, as seen in Fig. 4. For instance, the 1-phenyl substituent attached on the core pyrazolo[3,4-*d*]pyrimidinone exhibits hydrophobic interactions with the side chains of Tyr385, Trp378 and Phe518, and π-arene interaction with the backbone of Gly526. The other 5-phenyl group appeared to be packed between the side chains of Leu531, Val116, Leu359 and Tyr355. The core pyrazolo[3,4-*d*]pyrimidinone shows π-arene interaction with Ala527. The thienylmethylidene hydrazinyl group appeared to be surrounded by Phe518, Val523 and Try355.

The postulated binding pose of **6a** demonstrated hydrophobic and H-bonding interactions with the binding site residues, as demonstrated in Fig. 5. For instance, the 1-phenyl substituent attached on the core pyrazolo[3,4-*d*]pyrimidinone exhibited hydrophobic interactions with the side chains of Val116 and Met113, and π-arene interaction with Leu359. The other 5-phenyl group is packed between the side chains of Phe518, Met522 and the backbone of Val523. The core pyrazolo[3,4-*d*]pyrimidinone shows hydrophobic interaction with Leu531 and backbone of Val116. The cyanoacetohydrazide displays H-bonding interactions with the side chain of Tyr385.

For the docking pose of **8**, the hydrazinylidene group shows H-bonding interaction with the side chain of Tyr355. The 1-phenyl group on the pyrazolo[3,4-*d*]pyrimidinone core is packed between Leu531 and Ala527. The other 5-phenyl group shows π-arene interaction with Phe518 and hydrophobic interaction with Met522. Also, the core pyrazolo[3,4-*d*]pyrimidinone exhibited π-arene interactions with Ser353 and hydrophobic interaction with Val523, as summarized in as shown in Fig. 6. Generally, these interactions outline of **8** pose is similar to its congeneric **6a** which sharing similar pyrazolo[3,4-*d*]pyrimidinone chemotype. This also rationalizes their similar docking fitness.

For the docking pose of **12** (Fig. 7), the ethyl sulfanylacetate group shows H-bonding interactions with the side chains of Tyr385 and Ser530. The diphenyl substituents and the core pyrazolo[4,3-e][1,2,4]triazolo[4,3-*a*]pyrimidinone appeared to be packed between the hydrophobic side chains of Trp387, Phe518, Gly526, Val523 and Ala527 from one side, and Leu359, Leu531 and Tyr355 from another side. This indicates favorable hydrophobic interactions. The core pyrazolo[4,3-e][1,2,4]triazolo[4,3-*a*]pyrimidin exhibits π-arene interaction with Ala527. In general, these interactions pattern of **12** pose is relatively comparable to its congeneric **2c** possessing similar chemotype scaffold.

2.3.2. In silico prediction of physicochemical properties, pharmacokinetic profile, drug likeness score and toxicities profiles

Detailed discussion of this section can be found in the (Supplementary Material). Based on the obtained results, we conclude

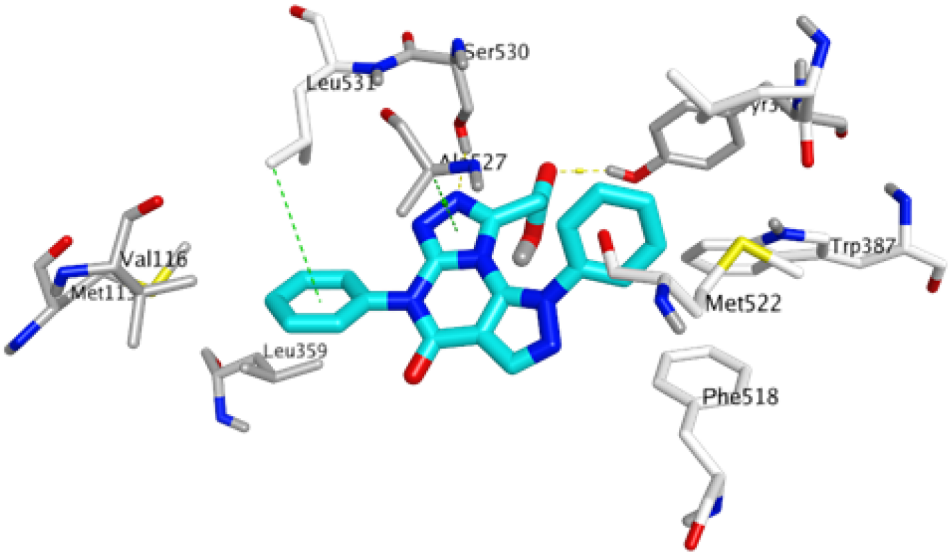

Fig. 3. The best-scored docking pose **2c** (cyan sticks) in the binding site of COX-2 enzyme (PDB: 5IKQ). Yellow and green broken lines indicate favorable H-bonding and π-arene interactions, respectively. Non-polar hydrogen atoms were omitted for clarity.

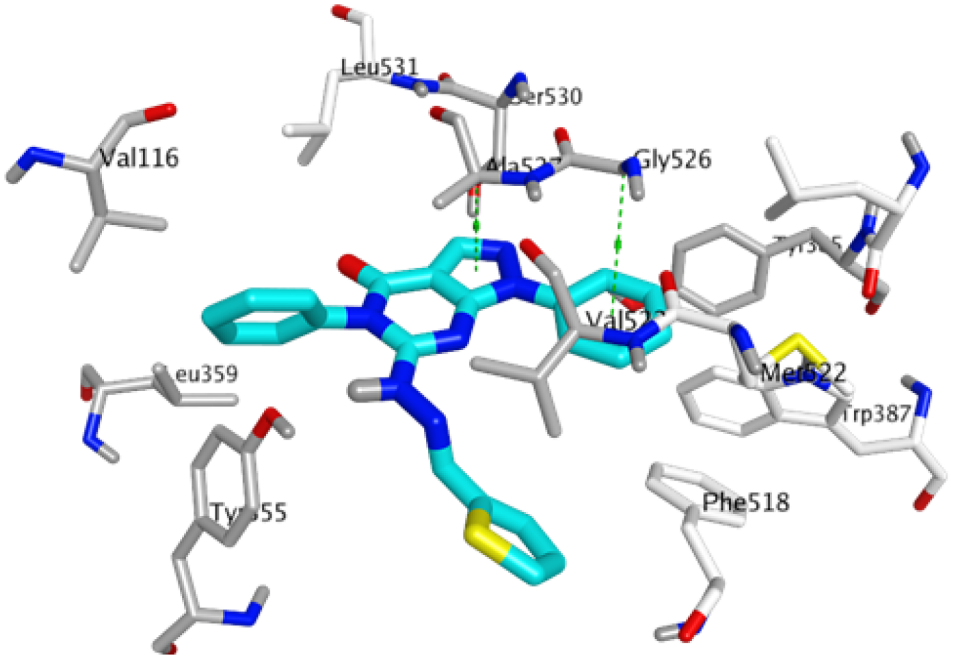

Fig. 4. The best-scored docking pose **3i** (cyan sticks) in the binding site of COX-2 enzyme (PDB: 5IKQ). Yellow and green broken lines indicate favorable H-bonding and π-arene interactions, respectively. Non-polar hydrogen atoms were omitted for clarity.

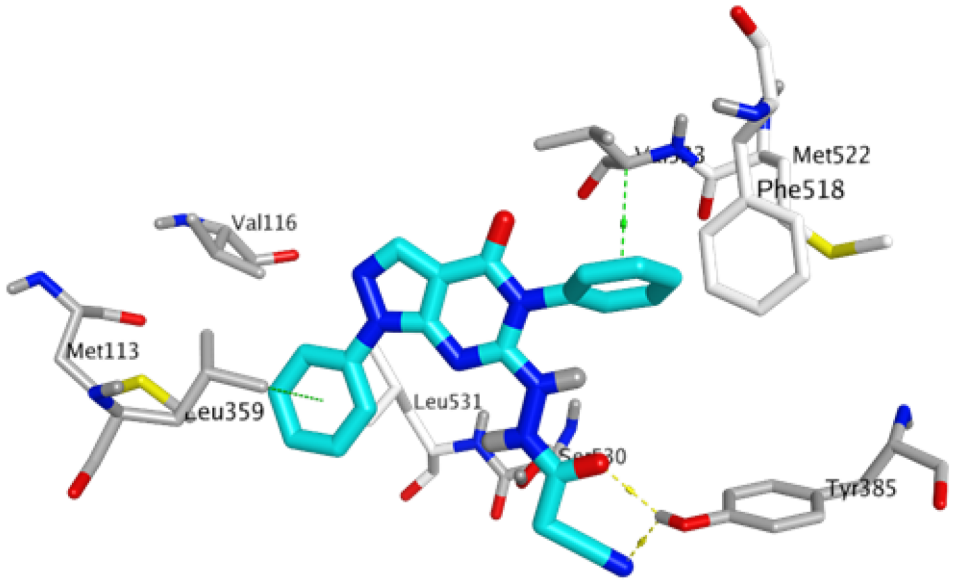

Fig. 5. The best-scored docking pose **6a** (cyan sticks) in the binding site of COX-2 enzyme (PDB: 5IKQ). Yellow and green broken lines indicate favorable H-bonding and π-arene interactions, respectively. Non-polar hydrogen atoms were omitted for clarity.

that most of the synthesized compounds showed reasonable drug-likeness scores and physicochemical properties. They also obeyed Lipinski's Rule of Five and showed acceptable pharmacokinetic parameters together with low toxicity profile.

3. Conclusion

The present study reported the synthesis and investigation of some new pyrazolopyrimidinones and pyrazolotriazolopyrimidinones as anti-inflammatory agents. The obtained results revealed that compounds **(2c, 6a, 8** and **12)** showed COX-2 inhibitory potency (IC_{50} = 0.58, 0.38, 0.74 and 0.29 μM, respectively) and selectivity indices (SI = 7.46, 12.23, 7.93 and 9.82, respectively) higher than celecoxib (IC_{50} = 0.78 μM and SI = 7.23). Moreover, compounds that showed promising *in vitro* results were further subjected to *in vivo* anti-inflammatory screening applying formalin induced paw edema and cotton-pellet induced granuloma assays using celecoxib and diclofenac sodium as reference drugs. The obtained *in vivo* data revealed that compounds (**2c, 2d, 3e, 3i, 6a, 8** and **12)** displayed anti-inflammatory activity (% AI = 64.3–78.6) higher than celecoxib (% AI = 46.4) in the acute model, whereas, compounds **(2c** and **6a)** possessed potent anti-inflammatory (% AI = 43.4 and 46.9) superior to both references (% AI = 8.6 and 36.1 for celecoxib and diclofenac sodium) in the chronic model. All the tested compounds exhibited safe gastrointestinal profile except for **(2c)**. Molecular docking experiments rationalized the observed i*n vitro* anti-inflammatory activity of **2c**, **3i**, **6a**, **8** and **12**. In silico predictions of the pharmacokinetic and drug-likeness properties suggested accepted profiles of the majority of compounds. Collectively,

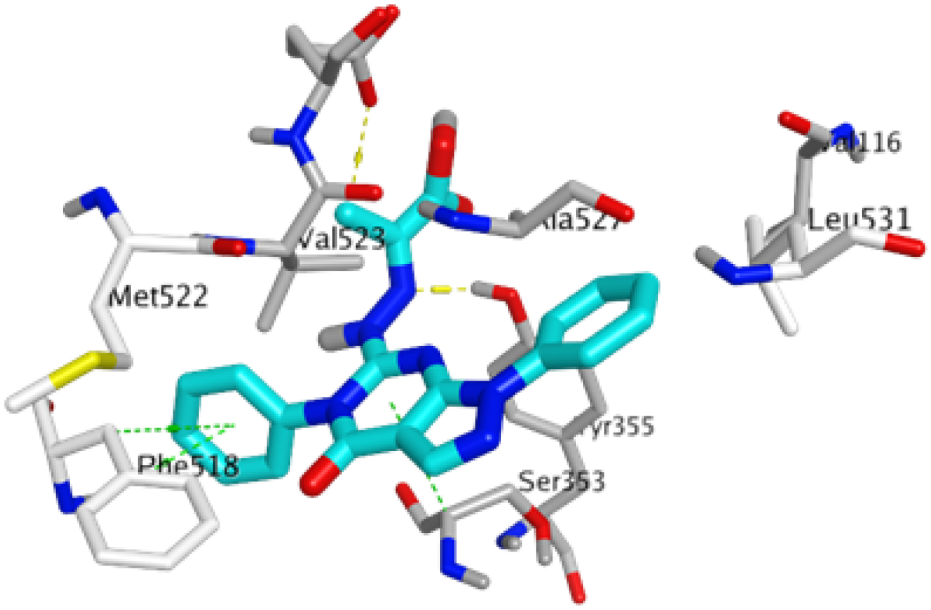

Fig. 6. The best-scored docking pose **8** (cyan sticks) in the binding site of COX-2 enzyme (PDB: 5IKQ). Yellow and green broken lines indicate favorable H-bonding and π-arene interactions, respectively. Non-polar hydrogen atoms were omitted for clarity.

the promising anti-inflammatory activity of the synthesized derivatives as well as their reduced ulcerogenic potential make them fruitful templates for further optimization and development of potent and safe anti-inflammatory agents.

4. Experimental

4.1. Chemistry

All reagents and solvents were purchased from commercial suppliers and were dried and purified when necessary by standard techniques.

Melting points were determined in open glass capillaries using Griffin melting point apparatus and are uncorrected. Infrared (IR) spectra were recorded on Perkine-Elmer RXIFT-IR spectrophotometer using KBr discs. ^{1}H NMR spectra were scanned on were run on Jeol spectrometer (500 MHz) at the Microanalytical Unit, Faculty of Science, Alexandria University, on Bruker high performance digital FT-NMR spectrometer avance III (400 MHz) at Faculty of Pharmacy, Cairo University and on Varian Mercury VX (300 MHz) spectrometer, Faculty of Science, Cairo University. ^{13}C NMR proton decoupled spectra were run on Jeol spectrometer (125 MHz) at the Microanalytical Unit. Faculty of Science, Alexandria University and on Varian Mercury VX (75 MHz) spectrometer, Faculty of Science, Cairo University, using deuterated dimethylsulfoxide (DMSO-d_6) as a solvent. The data were reported as chemical shifts or δ values (ppm) relative to

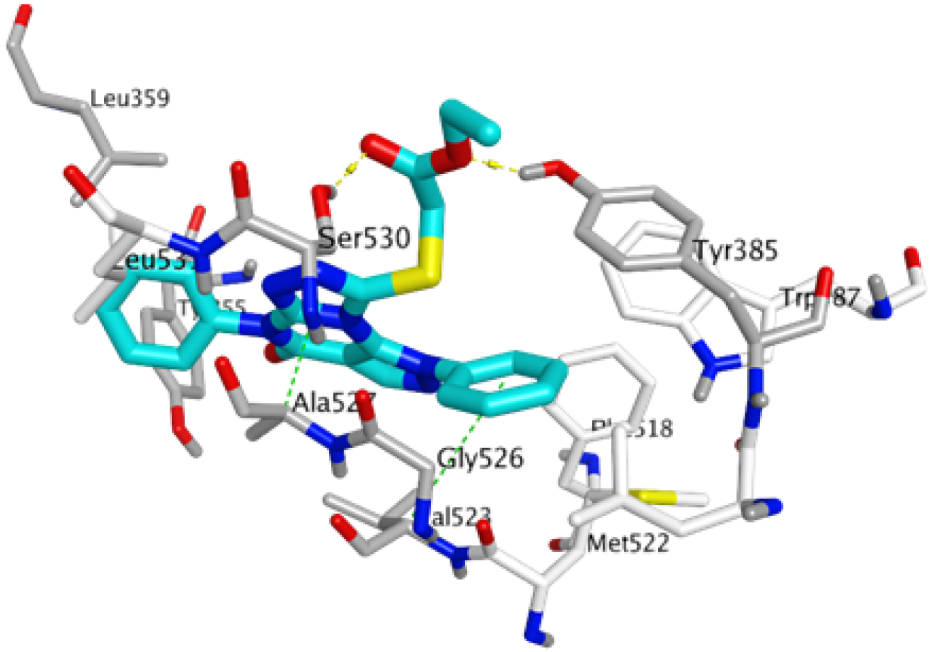

Fig. 7. The best-scored docking pose **12** (cyan sticks) in the binding site of COX-2 enzyme (PDB: 5IKQ). Yellow and green broken lines indicate favorable H-bonding and π-arene interactions, respectively. Non-polar hydrogen atoms were omitted for clarity.

tetramethylsilane (TMS) as internal standard. The type of signal was indicated by one of the following abbreviations: s = singlet, d = doublet, t = triplet, q = quartet, m = multiplet and dd = doublet of doublet. Mass spectra were run on a gas chromatograph/mass spectrophotometer Shimadzu GCMS/QP-2010 plus (70 eV) at the faculty of Science, Al-Azhar University. Relative intensity % corresponding to the most characteristic fragments were recorded. Microanalyses were performed at the Microanalytical Unit, Faculty of Science, Cairo University, Egypt and the found values were within ± 0.4% of the theoretical values. Follow up of the reactions and checking the purity of the compounds was made by thin layer chromatography (TLC) on silica gel-precoated aluminum sheets (Type 60 GF254; Merck; Germany) and the spots were detected by exposure to iodine vapour or UV lamp at λ. 254 nm for few seconds.

4.1.1. 4.1.1. 8-Substituted-1,5-diphenyl-1H-pyrazolo[4,3-e][1,2,4]triazolo[4,3-a]pyrimidin-4(5H)-ones (2a-d)

4.1.1.1. General method for preparation of ***8-substituted-1,5-diphenyl-1H-pyrazolo[4,3-e][1,2,4]triazolo[4,3-a]pyrimidin-4(5H)-ones (2a,b)***. A mixture of the hydrazine derivative **1** (0.32 g, 1 mmol) and glacial acetic acid or propanoic acid (5 ml) was heated under reflux for 3 h. The reaction mixture was concentrated under reduced pressure, left to cool and then poured into ice-cold water, neutralized with (10%) sodium hydroxide solution. Then the precipitated product was filtered, washed with water, dried and crystallized from ethanol. Physical and spectral data for **2a,b** are listed below.

4.1.1.1.1. ***8-Methyl-1,5-diphenyl-1H-pyrazolo[4,3-e][1,2,4]triazolo[4,3-a]pyrimidin-4(5H)-one (2a)***. Yield: 87%; Mp: 210 °C as reported [29]. IR (KBr, cm^{-1}): 3055, 3020, 2970, 2931, 2850 (CH); 1707 (C═O); 1594 (C═N); 1531, 1504 (C═C). ^{1}H NMR (300 MHz, DMSO-d_6) δ 2.45 (s, 3H, CH_3); 7.38–7.62 (m, 8H, phenyl-H); 8.15 (d, J = 7.8 Hz, 2H, phenyl $C_{2,6}$-H); 8.33 (s, 1H, pyrazolotriazolopyrimidinone C_3-H). MS (*m/z*, %): 342.65 ($M^{+\cdot}$, 3); 334 (100); 287 (38); 205 (9); 180 (7); 150 (7); 143 (6); 116 (19); 97 (12); 95 (17); 91 (17); 77 (45); 69 (21); 63 (14); 51 (36); 45 (31). Anal. Calcd for $C_{19}H_{14}N_6O$ (342.35): C, 66.66; H, 4.12; N, 24.55. Found: C, 66.84; H, 4.19; N, 24.78.

4.1.1.1.2. 8-Ethyl-1,5-diphenyl-1H-pyrazolo[4,3-e][1,2,4]triazolo [4,3-a]pyrimidin-4(5H)-one (2b). Yield: 69%; Mp: > 300 °C. IR (KBr, cm^{-1}): 3062, 2988, 2943, 2870 (C−H); 1707 (C═O); 1581 (C═N); 1553, 1532, 1496 (C═C). ^{1}H NMR (400 MHz, DMSO-d_6) δ 0.91 (t, J = 7.3 Hz, 3H, $CH_2\underline{CH_3}$); 1.80 (q, J = 7.3 Hz, 2H, $\underline{CH_2}CH_3$); 7.40–7.80 (m, 10*H*, phenyl-H); 8.46 (s, 1H, pyrazolotriazolopyrimidinone C_3-H). Anal. Calcd for $C_{20}H_{16}N_6O$ (356.38): C, 67.40; H, 4.53; N, 23.58. Found: C, 67.64; H, 4.67; N, 23.74.

4.1.1.2. ***2-(4-Oxo-1,5-diphenyl-4,5-dihydro-1H-pyrazolo[4,3-e][1,2,4]triazolo[4,3-a]pyrimidin-8-yl)acetic acid (2c)***. A mixture of the hydrazine derivative **1** (0.32 g, 1 mmol) and malonic acid (0.20 g, 2 mmol) in the presence of a catalytic amount of p-toluenesulphonic acid was heated in an oil bath at 200 °C for 1 h. The reaction mixture was allowed to cool to room temperature, triturated with ethanol, the separated product was filtered, washed with ethanol, dried and crystallized from ethanol. Yield: 50%; Mp: 293–295 °C. IR (KBr, cm^{-1}): 3442–3214 (OH); 3088, 3063 (CH); 1715, 1698 (C═O); 1618 (C═N); 1592, 1548, 1524, 1493 (C═C). ^{1}H NMR (300 MHz, DMSO-d_6) δ 2.48 (s, 2H, CH_2); 7.24–7.78 (m, 8H, phenyl-H); 8.09 (d, J = 8.1 Hz, 2H, phenyl $C_{2,6}$-H); 8.44 (s, 1H, pyrazolotriazolopyrimidinone C_3-H); 10.50 (s, 1H, carboxylic OH, D_2O exchangeable). MS (*m/z*, %):387.30 ($M^{+\cdot}$ + 1, 1); 386.59 ($M^{+\cdot}$, 3); 341 (20); 303 (53); 196 (56); 190 (54); 184 (28); 168. (40); 167 (51); 156 (55); 145 (50); 142. (47); 141 (94); 135 (29); 129 (79); 123 (20); 118 (42); 116 (32); 102 (48); 91 (57); 90 (64); 89 (22); 57 (99); 51 (79); 44 (100). Anal. Calcd for $C_{20}H_{14}N_6O_3$ (386.36): C, 62.17; H, 3.65; N, 21.75. Found: C, 62.41; H, 3.63; N, 21.94.

4.1.1.3. ***8-{2-[(2,6-Dichlorophenyl)amino]benzyl}-1,5-diphenyl-1H-pyrazolo[4,3-e][1,2,4]triazolo[4,3-a]pyrimidin-4(5H)-one (2d)***. A mixture of the hydrazine derivative **1** (0.32 g, 1 mmol), diclofenac acid (0.30 g, 1 mmol) and N,N′-dicyclohexylcarbodiimide (DCC) (0.41 g, 2 mmol) in methylene chloride (10 ml) was stirred at room temperature for 24 h. The reaction mixture was filtered then the solvent was evaporated under reduced pressure. The residual product was triturated with methanol and the separated product was filtered, washed with methanol, dried and crystallized from methanol. Yield: 55%; Mp: 274–278 °C. IR (KBr, cm^{-1}): 3251 (NH); 3063, 2927, 2854 (CH); 1704 (C═O); 1580 (C═N); 1547, 1498, 1450 (C═C). ^{1}H NMR (300 MHz, DMSO-d_6) δ 3.22 (s, 2H, CH_2); 6.20–7.84 (m, 18H, phenyl-H and NH); 8.50 (s, 1H, pyrazolotriazolopyrimidinone C_3-H). ^{13}C NMR spectrum (125 MHz, DMSO-d_6) δ 30.40 (CH_2); 104.83 (pyrazolotriazolopyrimidinone C_{3a}); 116.88, 121.09, 125.39, 126.23, 128.21, 129.39, 129.51, 129.58, 129.95, 130.46, 130.98, 131.07, 131.53, 135.53, 137.77, 138.43, 139.33, 139.58 (three phenyl C and dichlorophenyl C); 140.44, 143.18, 146.35, 151.81, 155.99 (pyrazolotriazolopyrimidinone $C_{3,4,5a,8,9a}$). MS (*m/z*, %):582 ($M^{+\cdot}$ + 4, 0.8); 580 ($M^{+\cdot}$ + 2, 5); 578 ($M^{+\cdot}$, 7.5); 246 (35); 244 (32); 233 (25); 219 (29); 207 (28); 178 (26); 144 (43); 122 (40); 117 (25); 108 (36); 104 (27); 103 (28); 102 (89); 96 (24); 83 (24); 78 (38); 76 (36); 74 (55); 64 (62); 57 (45); 51 (100); 50 (28); 45 (40); 44 (94). Anal. Calcd for $C_{31}H_{21}Cl_2N_7O$ (578.45): C, 64.37; H, 3.66; N, 16.95. Found: C, 64.51; H, 3.64; N, 17.21.

4.1.2. General procedure for ***6-{2-(Substituted methylidene)}hydrazinyl-1,5-diphenyl-1H-pyrazolo[3,4-d]pyrimidin-4(5H)-ones (3a-l)***

A mixture of the hydrazine derivative **1** (0.32 g, 1 mmol) and an equimolar amount of appropriate aldehyde in absolute ethanol (10 ml) was heated under reflux for 2 h. The reaction mixture was left to cool to attain room temperature then the separated product was filtered, washed with ethanol, dried and recrystallized from the proper solvent. Physical and spectral data for **3a-l** are listed below.

4.1.2.1. 6-{2-[(1,3-Diphenyl-1H-pyrazol-4-yl)methylene]hydrazinyl}-1,5-diphenyl-1,5-dihydro-4H-pyrazolo[3,4-d]pyrimidin-4-one (3a). Crystallization solvent: Ethanol. Yield: 70%; Mp: 270–272 °C. IR (KBr, cm^{-1}): 3287 (NH); 3052, 2906, 2869 (CH);1694 (C═O);1596 (C═N); 1543, 1499 (C═C). Anal. Calcd for $C_{33}H_{24}N_8O$ (548.60): C, 72.25; H, 4.41; N, 20.43. Found: C, 72.64; H, 4.48; N, 20.60.

4.1.2.2. 6-{2-[(3-(4-Bromophenyl)-1-phenyl-1H-pyrazol-4-yl)methylene]hydrazinyl}-1,5-diphenyl-1,5-dihydro-4H-pyrazolo[3,4-d]pyrimidin-4-one (3b). Crystallization solvent: Ethanol. Yield: 78%; Mp: 240–242 °C. IR (KBr, cm^{-1}): 3309 (NH); 3049 (CH); 1693 (C═O); 1597 (C═N); 1542, 1499 (C═C). Anal. Calcd for $C_{33}H_{23}BrN_8O$ (627.49): C, 63.16; H, 3.69; N, 17.86. Found: C, 63.34; H, 3.71; N, 18.02.

4.1.2.3. 6-{2-[(3-(4-Chlorophenyl)-1-phenyl-1H-pyrazol-4-yl)methylene]hydrazinyl}-1,5-diphenyl-1,5-dihydro-4H-pyrazolo[3,4-d]pyrimidin-4-one (3c). Crystallization solvent: Ethanol. Yield: 76%; Mp: 249–251 °C. IR (KBr, cm^{-1}): 3190 (NH); 3125, 3052 (CH); 1701 (C═O); 1667 (C═N); 1597, 1542, 1500 (C═C). ^{1}H NMR (400 MHz, DMSO-d_6) δ 7.34–7.94 (m, 17H, phenyl-H); 8.20 (s, 1H, N = CH); 8.27 (d, J = 7.8 Hz, 2H, phenyl $C_{2,6}$-H); 8.36 (s,1H, pyrazolopyrimidinone C_3-H); 8.68 (s, 1H, pyrazole C_5-H); 9.93 (s, 1H, NH, D_2O exchangeable). Anal. Calcd for $C_{33}H_{23}ClN_8O$ (583.04): C, 67.98; H, 3.98; N, 19.22. Found: C, 68.13; H, 4.02; N, 19.51.

4.1.2.4. 6-{2-[(3-(4-Methoxyphenyl)-1-phenyl-1H-pyrazol-4-yl)methylene]hydrazinyl}-1,5-diphenyl-1,5-dihydro-4H-pyrazolo[3,4-d]pyrimidin-4-one (3d). Crystallization solvent: Ethanol. Yield: 77%; Mp: 251–253 °C. IR (KBr, cm^{-1}): 3200 (NH); 3063, 2999, 2831 (CH); 1677 (C═O); 1600 (C═N); 1534, 1462 (C═C); 1250, 1054 (C−O−C). Anal.

Calcd for $C_{34}H_{26}N_8O_2$ (578.62): C, 70.58; H, 4.53; N, 19.37. Found: C, 70.81; H, 4.62; N, 19.60.

4.1.2.5. 6-{2-[(5-Chloro-3-methyl-1-phenyl-1H-pyrazol-4-yl)methylene] hydrazinyl}-1,5-diphenyl-1,5-dihydro-4H-pyrazolo[3,4-d]pyrimidin-4-one (3e). Crystallization solvent: Dioxane. Yield: 69%; Mp: 243–245 °C. IR (KBr, cm^{-1}): 3283 (NH); 3057, 2974, 2918 (CH); 1703 (C=O); 1598 (C=N); 1542, 1497 (C=C). ^{1}H NMR (500 MHz, DMSO-d_6) δ 2.62 (s, 3H, CH_3); 7.28–7.61 (m, 13H, phenyl-H); 8.15 (s, 1H, N = CH); 8.32 (s, 1H, pyrazolopyrimidinone C_3-H); 8.38 (d, J = 7.7 Hz, 2H, phenyl $C_{2,6}$-H); 9.82 (s, 1H, NH, D_2O exchangeable). MS (*m/z*, %): 522.80 ($M^{+\cdot}$ + 2, 1.40); 520.47 ($M^{+\cdot}$, 4.15); 405 (14); 302 (28); 213 (15); 198 (20); 187 (20); 186 (22); 184 (20); 183 (35); 128 (35); 118 (12); 117 (23); 116 (10); 115 (17); 92 (34); 83 (28); 77 (100); 76 (30); 71 (22); 63 (16); 60 (17); 57 (22); 56 (29); 54 (11); 51 (39); 50 (27); 45 (17); 44 (45); 43 (36). Anal. Calcd for $C_{28}H_{21}ClN_8O$ (520.97): C, 64.55; H, 4.06; N, 21.51. Found: C, 64.79; H, 4.12; N, 21.85.

4.1.2.6. 6-{2-[(3,5-Dimethyl-1-phenyl-1H-pyrazol-4-yl) methylidene] hydrazinyl}-1,5-diphenyl-1H-pyrazolo[3,4-d]pyrimidin-4(5H)-one (3f). Crystallization solvent: Dioxane. Yield: 72%; Mp: 245–247 °C. IR (KBr, cm^{-1}): 3381, 3306 (NH); 3098, 3059, 2965, 2918, 2870 (CH); 1696 (C=O); 1596 (C=N); 1543, 1498 (C=C). ^{1}H NMR (500 MHz, DMSO-d_6) δ 2.43, 2.45 (2s, each 3H, 2 CH_3); 7.27–7.62 (m, 13H, phenyl-H); 8.14 (s, 1H, N = CH); 8.32 (s, 1H, pyrazolopyrimidinone C_3-H); 8.39 (d, J = 7.7 Hz, 2H, phenyl $C_{2,6}$-H); 9.45 (s, 1H, NH, D_2O exchangeable). ^{13}C NMR spectrum (125 MHz, DMSO-d_6) δ 11.86, 13.84 (2 CH_3); 102.15 (pyrazolopyrimidinone C_{3a}) 114.26 (pyrazole C_4); 120.39, 125.23, 126.42, 128.30, 129.47, 129.75, 130.19, 130.23, 130.63 (three phenyl $C_{2\text{-}6}$); 134.60, 137.08, 139.33, 139.71, 140.00 (three phenyl C_1, pyrazolopyrimidinone C_3 and pyrazole C_5); 143.34, 148.41, 151.50, 153.31, 157.91 (pyrazolopyrimidinone $C_{4,6,7a}$, pyrazole C_3 and N=CH). Anal. Calcd for $C_{29}H_{24}N_8O$ (500.55): C, 69.58; H, 4.83; N, 22.39. Found: C, 69.72; H, 4.90; N, 22.67.

4.1.2.7. 6-{2-(Pyridin-3-ylmethylidene)}hydrazinyl-1,5-diphenyl-1H-pyrazolo[3,4-d]pyrimidin-4(5H)-one (3g). Crystallization solvent: Dioxane. Yield: 69%; Mp: 259–260 °C. IR (KBr, cm^{-1}): 3290 (NH); 3053, 3008 (CH); 1700 (C=O); 1596 (C=N); 1539, 1496 (C=C). ^{1}H NMR (400 MHz, DMSO-d_6) δ 7.41–7.67 (m, 9H, phenyl-H and pyridine C_2-H); 8.04 (d, J = 7.9, 1H, pyridine C_4-H); 8.21 (s, 1H, N=CH); 8.33 (s, 1H, pyrazolopyrimidinone C_3-H); 8.38 (d, J = 7.8 Hz, 2H, phenyl $C_{2,6}$-H); 8.59 (dd, J = 4.7, 1.5, 1H, pyridine C_5-H); 8.76 (s, 1H, pyridine C_6-H); 10.20 (s, 1H, NH, D_2O exchangeable). Anal. Calcd for $C_{23}H_{17}N_7O$ (407.43): C, 67.80; H, 4.21; N, 24.06. Found: C, 68.04; H, 4.29; N, 24.30.

4.1.2.8. 6-{2-(Furylmethylidene)}hydrazinyl-1,5-diphenyl-1H-pyrazolo [3,4-d]pyrimidin-4(5H)-one (3h). Crystallization solvent: Ethanol. Yield: 67%; Mp: 193–194 °C. IR (KBr, cm^{-1}): 3392, 3287 (NH); 3055, 2970, 2932 (CH); 1704 (C=O); 1594 (C=N); 1529, 1502, 1478 (C=C). Anal. Calcd for $C_{22}H_{16}N_6O_2$ (396.40): C, 66.66; H, 4.07; N, 21.20. Found: C, 66.78; H, 4.15; N, 21.47.

4.1.2.9. 6-{2-(Thienylmethylidene)}hydrazinyl-1,5-diphenyl-1H-pyrazolo [3,4-d]pyrimidin-4(5H)-one (3i). Crystallization solvent: Ethanol. Yield: 63%; Mp: 245–249 °C. IR (KBr, cm^{-1}): 3288 (NH); 3066, 2908 (CH); 1697 (C=O); 1596 (C=N); 1540, 1495 (C=C); 1289, 1058 (C–S–C). Anal. Calcd for $C_{22}H_{16}N_6OS$ (412.47): C, 64.06; H, 3.91; N, 20.38; S, 7.77. Found: C, 64.32; H, 3.98; N, 20.61; S, 7.84.

4.1.2.10. ***6-{2-(Substituted benzylidene)}hydrazinyl-1,5-diphenyl-1H-pyrazolo[3,4-d]pyrimidin-4(5H)-one (3j-l)*** *[29]*

4.1.2.10.1. 6-{2-(Benzylidene)}hydrazinyl-1,5-diphenyl-1H-pyrazolo [3,4-d]pyrimidin-4(5H)-one (3j). Mp: 88 °C; reported 92 °C [29].

4.1.2.10.2. 6-{2-(4-Methoxybenzylidene)}hydrazinyl-1,5-diphenyl-1H-pyrazolo[3,4-d]pyrimidin-4(5H)-one (3k). Mp: 87 °C as reported [29].

4.1.2.10.3. 6-{2-(4-Chlorobenzylidene)}hydrazinyl-1,5-diphenyl-1H-pyrazolo[3,4-d]pyrimidin-4(5H)-one (3l). Mp: 80 °C; reported 70 °C [29].

4.1.3. General procedure for ***7-Acetyl-8-aryl-1,5-diphenyl-7,8-dihydro-1H-pyrazolo[4,3-e][1,2,4]triazolo[4,3-a]pyrimidin-4(5H)-ones (4a-c)***

A suspension of the hydrazone derivative **3j-l** (1 mmol) in acetic anhydride (2 ml) was heated under reflux for 8 h. The reaction mixture was left to cool and poured into ice-cold water. The separated product was filtered, washed with water, dried and crystallized from ethanol. Physical and spectral data for **4a-c** are listed below.

4.1.3.1. ***7-Acetyl-1,5,8-triphenyl-7,8-dihydro-1H-pyrazolo[4,3-e][1,2,4]triazolo[4,3-a]pyrimidin-4(5H)-one (4a)***. Yield: 63%; Mp: 268–269 °C. IR (KBr, cm^{-1}): 3093, 3066, 3033, 2937 (CH); 1719, 1632 (C=O); 1572 (C=N); 1556, 1495, 1461 (C=C). ^{1}H NMR (300 MHz, DMSO-d_6) δ 1.77 (s, 3H, CH_3); 6.77 (d, J = 7.2 Hz, 2H, phenyl-H); 6.88 (s, 1H, pyrazolotriazolopyrimidinone C_8-H); 7.06–7.60 (m, 13H, phenyl-H); 8.12 (s, 1H, pyrazolotriazolopyrimidinone C_3-H ^{13}C NMR spectrum (125 MHz, DMSO-d_6) δ 21.06 (CH_3); 77.05 (pyrazolotriazolopyrimidinone C_8); 100.43 (pyrazolotriazolopyrimidinone C_{3a}); 126.74, 126.97, 128.78, 129.45, 129.56, 129.70, 129.77, 130.19, 130.32 (three phenyl $C_{2\text{-}6}$); 134.83, 135.52, 137.16, 139.16, 140.36 (three phenyl C_1 and pyrazolotriazolopyrimidinone $C_{5a,9a}$); 165.87 (acetyl C=O). Anal. Calcd for $C_{26}H_{20}N_6O_2$ (448.48): C, 69.63; H, 4.49; N, 18.74. Found: C, 69.89; H, 4.53; N, 19.01.

4.1.3.2. ***7-Acetyl-8-(4-chlorophenyl)-1,5-diphenyl-7,8-dihydro-1H-pyrazolo[4,3-e][1,2,4]triazolo[4,3-a]pyrimidin-4(5H)-one (4b)***. Yield: 66%; Mp: 235–236 °C. IR (KBr, cm^{-1}): 3067, 3094, 2940 (CH); 1718, 1631 (C=O); 1567 (C=N); 1493, 1463 (C=C). ^{1}H NMR (300 MHz, DMSO-d_6) δ 2.07 (s, 3H, CH_3); 6.89 (s, 1H, pyrazolotriazolopyrimidinone C_8-H); 7.08–7.83 (m, 14H, phenyl-H); 8.59 (s, 1H, pyrazolotriazolopyrimidinone C_3-H). Anal. Calcd for $C_{26}H_{19}ClN_6O_2$ (482.92): C, 64.66; H, 3.97; N, 17.40. Found: C, 64.92; H, 3.99; N, 17.57.

4.1.3.3. ***7-Acetyl-8-(4-methoxyphenyl)-1,5-diphenyl-7,8-dihydro-1H-pyrazolo[4,3-e][1,2,4]triazolo[4,3-a]pyrimidin-4(5H)-one (4c)***. Yield: 65%; Mp: 222–224 °C. IR (KBr, cm^{-1}): 3076, 3035, 3009, 2953, 2932, 2835 (CH); 1702, 1627 (C=O); 1552 (C=N); 1497, 1469 (C=C); 1249, 1027 (C–O–C). ^{1}H NMR (500 MHz, DMSO-d_6) δ 1.77 (s, 3H, CH_3); 3.70 (s, 3H, OCH_3); 6.62, 6.67 (2d, J = 8.8 Hz, 4H, methoxy phenyl-H); 6.83 (s, 1H, pyrazolotriazolopyrimidinone C_8-H); 7.13–7.89 (m, 10*H*, phenyl-H); 8.30 (s, 1H, pyrazolotriazolopyrimidinone C_3-H). Anal. Calcd for $C_{27}H_{22}N_6O_3$ (478.50): C, 67.77; H, 4.63; N, 17.56. Found: C, 68.01; H, 4.69; N, 17.68.

4.1.3.4. 1,5-Diphenyl-1H-pyrazolo[4,3-e][1,2,4]triazolo[4,3-a] pyrimidine-4,8(5H,7H)-dione (5). A mixture of the hydrazine derivative **1** (0.32g, 1 mmol) and urea (0.48 g, 8 mmol) was heated in an oil bath at 200 °C for 2 h. The reaction mixture was allowed to cool to room temperature and the residue was treated with hot water to wash off excess urea. The separated product was filtered, washed with water, dried then crystallized from dioxane. Yield: 33%, Mp. > 300 °C. IR (KBr, cm^{-1}): 3201 (NH); 3053, 2956, 2831 (CH); 1760, 1704 (C=O); 1601 (C=N); 1530, 1497 (C=C). ^{1}H NMR (300 MHz, DMSO-d_6) δ 7.35–7.58 (m, 8H, phenyl-H); 8.02 (d, J = 8.1 Hz, 2H, phenyl $C_{2,6}$-H); 8.30 (s, 1H, pyrazolotriazolopyrimidinone C_3-H); 13.00 (s, 1H, NH, D_2O exchangeable). Anal. Calcd for $C_{18}H_{12}N_6O_2$ (344.33): C, 62.79; H, 3.51; N, 24.41. Found: C, 63.04; H, 3.50; N, 24.68.

*4.1.4. General procedure for compounds (**6a-c**)*

4.1.4.1. 2-Cyano-N'-(4-oxo-1,5-diphenyl-4,5-dihydro-1*H*-pyrazolo [3,4-*d*] pyrimidin-6-yl)acetohydrazide (6a)
4.1.4.2. Ethyl 2-oxo-2-{2-(4-oxo-1,5-diphenyl-4,5-dihydro-1*H*-pyrazolo [3,4-*d*] pyrimidin-6-yl)hydrazinyl}acetate (6b)
4.1.4.3. Ethyl 3-oxo-3-{2-(4-oxo-1,5-diphenyl-4,5-dihydro-1*H*-pyrazolo [3,4-*d*] pyrimidin-6-yl)hydrazinyl}propanoate (6c)

A mixture of the hydrazine derivative **1** (0.32 g, 1 mmol) and ethyl cyanoacetate, diethyl oxalate or diethyl malonate (2 ml) was heated under reflux for 15 min. to 4 h. The reaction mixture was left to cool to room temperature and diluted with ethanol (3 ml). The separated crystals were filtered, washed with ethanol, dried and recrystallized from ethanol. Physical and spectral data for **6a-c** are listed below.

4.1.4.1. 2-Cyano-N′-(4-oxo-1,5-diphenyl-4,5-dihydro-1H-pyrazolo[3,4-d] pyrimidin-6-yl)acetohydrazide (6a). Reaction time: 2 h; Yield: 47%; Mp: 161–163 °C. IR (KBr, cm^{-1}): 3410, 3251 (NH); 3117, 3040, 2938, 2911 (CH); 2258 (CN); 1708, 1696 (C═O); 1596 (C═N); 1551, 1500, 1491, 1421 (C═C). ^{1}H NMR (300 MHz, DMSO-d_6) δ 3.82 (s, 2H, CH_2); 7.33–7.62 (m, 8H, phenyl-H); 8.12 (d, J = 7.8 Hz, 2H, phenyl $C_{2,6}$-H); 8.21 (s, 1H, pyrazolopyrimidinone C_3-H); 8.52, 10.31 (2s, 2H, 2NH, D_2O exchangeable). Anal. Calcd for $C_{20}H_{15}N_7O_2$ (385.38): C, 62.33; H, 3.92; N, 25.44. Found: C, 62.50; H, 3.95; N, 25.62.

4.1.4.2. Ethyl 2-oxo-2-{2-(4-oxo-1,5-diphenyl-4,5-dihydro-1H-pyrazolo [3,4-d]pyrimidin-6-yl)hydrazinyl}acetate (6b). Reaction time: 4 h; Yield: 72%; Mp: 214–215 °C. IR (KBr, cm^{-1}): 3354, 3241 (NH); 3101, 3067, 2972 (CH); 1756, 1689 (C═O); 1598 (C═N); 1551, 1526, 1500 (C═C); 1215, 1077 (C−O−C). ^{1}H NMR (300 MHz, DMSO-d_6) δ 1.30 (t, J = 6.8 Hz, 3H, $CH_2\underline{CH_3}$); 4.34 (q, J = 6.8 Hz, 2H, $\underline{CH_2}CH_3$); 7.35–7.61 (m, 8H, phenyl- H); 8.13 (d, J = 7.8 Hz, 2H, phenyl $C_{2,6}$-H); 8.18 (s, 1H, pyrazolopyrimidinone C_3-H); 8.67, 10.93 (2s, each 1H, 2NH, D_2O exchangeable). Anal. Calcd for $C_{21}H_{18}N_6O_4$ (418.41(: C, 60.28; H, 4.34; N, 20.09. Found: C, 60.43; H, 4.41; N, 20.21.

4.1.4.3. Ethyl 3-oxo-3-{2-(4-oxo-1,5-diphenyl-4,5-dihydro-1H-pyrazolo [3,4-d]pyrimidin-6-yl)hydrazinyl}propanoate (6c). Reaction time: 15 min.; Yield: 60%; Mp: 243–244 °C. IR (KBr, cm^{-1}): 3411, 3264 (NH); 3050, 2996, 2977, 2905 (CH); 1740, 1707 (C═O); 1595 (C═N); 1558, 1473, (C═C); 1255, 1068 (C−O−C). ^{1}H NMR (300 MHz, DMSO-d_6) δ 1.16 (t, J = 7.0 Hz, 3H, $CH_2\underline{CH_3}$); 3.36 (s, 2H, CH_2); 4.08 (q, J = 7.0 Hz, 2H, $\underline{CH_2}CH_3$) 7.34–7.64 (m, 8H, phenyl-H); 8.14, 8.18 (m, 3H, 2H, phenyl $C_{2,6}$-H and pyrazolopyrimidinone C_3-H); 8.46, 10.12 (2s, each 1H, 2NH, D_2O exchangeable). Anal. Calcd for $C_{22}H_{20}N_6O_4$ (432.43): C, 61.10; H, 4.66; N, 19.43. Found: C, 61.34; H, 4.71; N, 19.70.

*4.1.5. General procedure for **6-{2-(2-Bromo-1-arylethylidene) hydrazinyl}-1,5-diphenyl-1H-pyrazolo[3,4-d]pyrimidin-4(5H)-ones (7a-d)***

A mixture of the hydrazine derivative **1** (0.32 g, 1 mmol) and the appropriate phenacyl bromide (1 mmol) in absolute ethanol (10 ml) was heated under reflux for 12 h. The separated light yellow product was filtered, washed with ethanol, dried and recrystallized from dimethylformamide. Physical and spectral data for **7a-d** are listed below.

4.1.5.1. 6-{2-(2-Bromo-1-phenylethylidene)hydrazinyl}-1,5-diphenyl-1H-pyrazolo[3,4-d]pyrimidin-4(5H)-one (7a). Yield: 60%; Mp: > 300 °C. IR (KBr, cm^{-1}): 3305, 3221 (NH); 3072 (CH); 1719 (C═O); 1596 (C═N); 1531, 1496, 1423 (C═C). Anal. Calcd for $C_{25}H_{19}BrN_6O$ (499.36): C, 60.13; H, 3.84; N, 16.83. Found: C, 60.40; H, 3.90; N, 16.97.

4.1.5.2. 6-{2-(2-Bromo-1-(4-bromophenyl)ethylidene)hydrazinyl}-1,5-diphenyl-1H-pyrazolo[3,4-d]pyrimidin-4(5H)-one (7b). Yield: 80%; Mp: 268–269 °C. IR (KBr, cm^{-1}): 3315, 3213 (NH); 3072 (CH); 1709 (C═O); 1594 (C═N); 1532, 1494 (C═C). ^{1}H NMR (400 MHz, DMSO-d_6) δ 3.72, 3.80 (2s, each 2H, CH_2, E and Z isomers); 6.97–8.42 (m, 30H, phenyl-H and pyrazolopyrimidinone C_3-H, E and Z isomers); 10.05, 10.15 (2s, each 1H, 2 NH, D_2O exchangeable, E and Z isomers). Anal. Calcd for $C_{25}H_{18}Br_2N_6O$ (578.26): C, 51.93; H, 3.14; N, 14.53. Found: C, 52.16; H, 3.19; N, 14.78.

4.1.5.3. 6-{2-(2-Bromo-1-(4-methylphenyl)ethylidene)hydrazinyl}-1,5-diphenyl-1H-pyrazolo[3,4-d]pyrimidin-4(5H)-one (7c). Yield: 66%; Mp: > 300 °C. IR (KBr, cm^{-1}): 3306, 3217 (NH); 3096, 3066, 2967, 2922 (CH); 1708 (C═O); 1595 (C═N); 1532, 1496 (C═C). MS (*m/z*, %): 515.80 ($M^{+\cdot}$ + 2, 13.9); 513.55 ($M^{+\cdot}$, 15); 452 (15); 440 (14); 328 (27); 218 (20); 203 (23); 199 (52); 193 (30); 169 (26); 143 (28); 140 (20); 130 (28); 114 (27); 109 (36); 108 (22); 97 (18); 91 (27); 89 (21); 84 (43); 82 (22); 74 (23); 73 (100); 60 (28); 56 (20); 52 (28); 46 (25); 44 (29); 42 (54). Anal. Calcd for $C_{26}H_{21}BrN_6O$ (513.39): C, 60.83; H, 4.12; N, 16.37. Found: C, 61.06; H, 4.19; N, 16.52.

4.1.5.4. 6-{2-(2-Bromo-1-(4-methoxyphenyl)ethylidene)hydrazinyl}-1,5-diphenyl-1H-pyrazolo[3,4-d]pyrimidin-4(5H)-one (7d). Yield: 70%; Mp: > 300 °C. IR (KBr, cm^{-1}): 3329, 3304 (NH); 3080, 2967, 2936, 2839 (CH); 1718 (C═O); 1599 (C═N); 1532, 1494 (C═C); 1058, 1249 (C−O−C). ^{1}H NMR (300 MHz, DMSO-d_6) δ 3.80, 3.82 (2s, each 3H, OCH_3, E and Z isomers); 3.90, 3.96 (2s, each 2H, CH_2, E and Z isomers); 6.83–8.41 (m, 30H, phenyl-H and pyrazolopyrimidinone C_3-H, E and Z isomers); 9.95, 10.09 (2s, each 1H, 2 NH, D_2O exchangeable, E and Z isomers). Anal. Calcd for $C_{26}H_{21}BrN_6O_2$ (529.39): C, 58.99; H, 4.00; N, 15.87. Found: C, 59.14; H, 4.07; N, 16.04.

4.1.6. 2-{2-(4-Oxo-1,5-diphenyl-4,5-dihydro-1H-pyrazolo[3,4-d] pyrimidin-6-yl)hydrazinylidene}propanoic acid (8)

An equimolar amount of the hydrazine derivative **1** (0.32 g, 1 mmol) and sodium pyruvate (0.12 g, 1 mmol) in ethanol (10 ml) containing (0.5 ml) glacial acetic acid was heated under reflux for 4 h. The reaction mixture was left to cool to attain room temperature where the sodium salt of the separated product was filtered, washed with ethanol and dried. A concentrated solution of the sodium salt in water (5 ml) was added to a stirred cold diluted hydrochloric acid then the precipitated product was filtered, washed with water, dried and crystallized from ethanol as yellow crystals. Yield: 60%, Mp. 238–239 °C. IR (KBr, cm^{-1}): 3420–3250 (OH, NH); 3057, 3010, 2908 (CH); 1715, 1690 (C═O); 1602 (C═N); 1537, 1497 (C═C). ^{1}H NMR (300 MHz, DMSO-d_6) δ 1.91 (s, 3H, CH_3); 7.35–7.62 (m, 9H, phenyl-H and NH); 8.23–8.25 (m, 3H, phenyl $C_{2,6}$-H and pyrazolopyrimidinone C_3-H); 12.27 (s, 1H, carboxylic OH, D_2O exchangeable). MS (*m/z*, %): 388.31 ($M^{+\cdot}$, 2); 343 (22); 329 (19); 303 (20); 302 (19); 186 (13); 129 (8); 119 (10); 103 (15); 91 (21); 77 (100); 65 (20); 55 (10); 51 (32); 44 (40). Anal. Calcd for $C_{20}H_{16}N_6O_3$ (388.38): C, 61.85; H, 4.15; N, 21.64. Found: C, 62.09; H, 4.11; N, 21.91.

*4.1.7. General procedure for **1-(4-Oxo-1,5-diphenyl-4,5-dihydro-1H-pyrazolo[3,4-d]pyrimidin-6-yl)-4-aryl thiosemicarbazides (9a-d)***

An equimolar amount of the hydrazine derivative **1** (0.32 g, 1 mmol) and the appropriate aryl isothiocyanate in methylene chloride (10 ml) was stirred at room temperature for 24 h. The separated white solid product was filtered, washed with diethyl ether, dried and recrystallized from ethanol. Physical and spectral data for **9a-d** are listed below.

4.1.7.1. 1-(4-Oxo-1,5-diphenyl-4,5-dihydro-1H-pyrazolo[3,4-d]pyrimidin-6-yl)-4-phenyl thiosemicarbazide (9a). Yield: 77%; Mp: > 300 °C. IR (KBr, cm^{-1}): 3337, 3238 (NH); 3104, 3054 (CH); 1678 (C═O); 1596 (C═N); 1549, 1499 (C═C); 1527; 1300, 1122, 970 (N−C═S). ^{1}H NMR (300 MHz, DMSO-d_6) δ 7.16–8.35 (m, 16H, phenyl-H and pyrazolopyrimidinone C_3-H); 8.74, 9.45, 9.65 (3s, each 1H, 3 NH,

D_2O exchangeable). Anal. Calcd for $C_{24}H_{19}N_7OS$ (453.52): C, 63.56; H, 4.22; N, 21.62; S, 7.07 Found: C, 63.69; H, 4.26; N, 21.89; S, 7.21.

4.1.7.2. 1-(4-Oxo-1,5-diphenyl-4,5-dihydro-1H-pyrazolo[3,4-d]pyrimidin-6-yl)-4-(4-chlorophenyl) thiosemicarbazide (9b). Yield: 90%; Mp: > 300 °C. IR (KBr, cm^{-1}): 3345, 3191 (NH); 3070, 2967 (CH); 1696 (C═O); 1596 (C═N); 1569, 1550, 1525, 1492, 1464 (C═C); 1499, 1249, 1097, 976 (N—C═S). Anal. Calcd for $C_{24}H_{18}ClN_7OS$ (487.96): C, 59.07; H, 3.72; N, 20.09; S, 6.57 Found: C, 59.22; H, 3.70; N, 20.32; S, 6.63.

4.1.7.3. 1-(4-Oxo-1,5-diphenyl-4,5-dihydro-1H-pyrazolo[3,4-d]pyrimidin-6-yl)-4-(4-methylphenyl) thiosemicarbazide (9c). Yield: 88%; Mp: > 300 °C. IR (KBr, cm^{-1}): 3348, 3201 (NH); 3070, 3035, 2965 (CH); 1695 (C═O); 1569 (C═N); 1527, 1494, 1464 (C═C); 1523, 1271, 1120, 976 (N—C═S). ^{1}H NMR (400 MHz, DMSO-d_6) δ 2.27 (s, 3H, CH_3); 7.09–7.61 (m, 12H, phenyl-H); 8.22 (s, 1H, pyrazolopyrimidinone C_3-H); 8.36 (d, J = 7.8 Hz, 2H, phenyl $C_{2,6}$-H); 8.75, 9.46, 9.62 (3s, each 1H, 3 NH, D_2O exchangeable). Anal. Calcd for $C_{25}H_{21}N_7OS$ (467.55): C, 64.22; H, 4.53; N, 20.97; S, 6.86 Found: C, 64.38; H, 4.59; N, 21.13; S, 6.94.

4.1.7.4. 1-(4-Oxo-1,5-diphenyl-4,5-dihydro-1H-pyrazolo[3,4-d]pyrimidin-6-yl)-4-(4-methoxyphenyl) thiosemicarbazide (9d). Yield: 89%; Mp: > 300 °C. IR (KBr, cm^{-1}): 3348, 3203 (NH); 3071, 2958, 2838 (CH); 1694 (C═O); 1596 (C═N); 1524, 1464 (C═C); 1502, 1257, 1122, 975 (N—C═S); 1264, 1011 (C—O—C). Anal. Calcd for $C_{25}H_{21}N_7O_2S$ (483.54): C, 62.10; H, 4.38; N, 20.28; S, 6.63 Found: C, 62.38; H, 4.42; N, 20.43; S, 6.72.

4.1.8. 1,5-Diphenyl-8-thioxo-7,8-dihydro-1H-pyrazolo[4,3-e][1,2,4] triazolo[4,3-a]pyrimidin-4(5H)-one (10)

A mixture of the hydrazine derivative **1** (0.32 g, 1 mmol) and phenyl isothiocyante (0.16 g, 0.14 ml, 1.2 mmol) in dry dioxane (7 ml) was heated under reflux for 14 h. The reaction mixture was allowed to cool to room temperature then poured into ice-cold water. The separated product was filtered, washed with water, dried and crystallized from ethanol. Yield: 63%, Mp. 209–210 °C reported 198–199 °C[29]. IR (KBr, cm^{-1}): 3376 (NH); 3059, 2910, 2780 (CH); 1703 (C═O); 1615 (C═N); 1551, 1493, 1453 (C═C); 1510, 1303, 1118 and 994 (N—C═S). ^{1}H NMR (500 MHz, DMSO-d_6) δ 7.42–7.56 (m, 10*H*, phenyl-H); 8.40 (s, 1H, pyrazolotriazolopyrimidinone C_3-H); 13.63 (s, 1H, NH, D_2O exchangeable). Anal. Calcd for $C_{18}H_{12}N_6OS$ (360.30): C, 59.99; H, 3.36; N, 23.32; S, 8.90 Found: C, 60.17; H, 3.40; N, 23.60; S, 8.91.

4.1.9. General procedure for 8-(Substituted sulfanyl)-1,5-diphenyl-1H-pyrazolo[4,3-e][1,2,4]triazolo[4,3-a]pyrimidin-4(5H)-ones (11a-c)

A mixture of the thioxo derivative **10** (0.36 g, 1 mmol), an equivalent amount of the proper alkylating reagent namely; methyl iodide, ethyl iodide or benzyl chloride and anhydrous potassium carbonate (0.17 g, 1.2 mmol) in dry dimethylformamide (5 ml) was stirred at room temperature for 24 h. The reaction mixture was poured into ice-cold water. The separated solid was filtered, washed with water, dried and crystallized from ethanol. Physical and spectral data for **11a-c** are listed below.

*4.1.9.1. **8-(Methylsulfanyl)-1,5-diphenyl-1H-pyrazolo[4,3-e][1,2,4] triazolo[4,3-a]pyrimidin-4(5H)-one (11a)***. Yield: 80%; Mp: 229–230 °C. IR (KBr, cm^{-1}): 3089, 3047, 2930 (CH); 1700 (C═O); 1576 (C═N); 1547, 1518, 1494 (C═C); 1261, 1076 (C—S—C). ^{1}H NMR (300 MHz, DMSO-d_6) δ 2.34 (s, 3H, S-CH_3); 7.43–7.75 (m, 10*H*, phenyl-H); 8.39 (s, 1H, pyrazolotriazolopyrimidinone C_3-H). Anal. Calcd for $C_{19}H_{14}N_6O_S$ (374.42): C, 60.95; H, 3.77; N, 22.45; S, 8.56 Found: C, 61.14; H, 3.73; N, 22.67; S, 8.67.

*4.1.9.2. **8-(Ethylsulfanyl)-1,5-diphenyl-1H-pyrazolo[4,3-e][1,2,4] triazolo[4,3-a]pyrimidin-4(5H)-one (11b)***. Yield: 87%; Mp: 178–179 °C. IR (KBr, cm^{-1}): 3100, 3064, 3004, 2967, 2932, 2874 (CH); 1706 (C═O); 1581 (C═N); 1551, 1523,1494 (C═C); 1250, 1080 (C—S—C). ^{1}H NMR (300 MHz, DMSO-d_6) δ 1.05 (t, J = 7.2 Hz, 3H, $CH_2\underline{CH_3}$); 2.82 (q, J = 7.2 Hz, 2H, $\underline{CH_2}$ CH_3); 7.54–7.67 (m, 10*H*, phenyl-H); 8.46 (s, 1H, pyrazolotriazolopyrimidinone C_3-H). ^{13}C NMR spectrum (75 MHz, DMSO-d_6) δ 14.00 (CH_3); 29.40 (S-CH_2); 104.49 (pyrazolotriazolopyrimidinone C_{3a}); 127.14, 128.84, 129.20, 129.62, 130.36, 134.89, 136.87, 138.78 (two phenyl-C); 139.29, 142.12, 151.86, 155.36, 160.10 (pyrazolotriazolopyrimidinone $C_{3,4,5a,8,9a}$). MS (*m/z*, %): 388.32 ($M^{+\cdot}$, 8); 355 (18); 327 (4); 287 (5); 183 (18); 143 (11); 103 (14); 91 (18); 77 (100); 69 (23); 65 (17); 55 (17); 51 (26); 44 (41); 43 (38); 40 (41). Anal. Calcd for $C_{20}H_{16}N_6OS$ (388.45): C, 61.84; H, 4.15; N, 21.63; S, 8.25 Found: C, 62.02; H, 4.19; N, 21.89; S, 8.41.

*4.1.9.3. **8-(Benzylsulfanyl)-1,5-diphenyl-1H-pyrazolo[4,3-e][1,2,4] triazolo[4,3-a]pyrimidin-4(5H)-one (11c)***. Yield: 75%; Mp: 216–218 °C. IR (KBr, cm^{-1}): 3035, 2952 (CH); 1712 (C═O); 1599, 1571 (C═N); 1496, 1457 (C═C); 1230, 1135 (C—S—C). Anal. Calcd for $C_{25}H_{18}N_6OS$ (450.52): C, 66.65; H, 4.03; N, 18.65; S, 7.12 Found: C, 66.87; H, 4.11; N, 18.89; S, 7.21.

4.1.10. Ethyl 2-(4-oxo-1,5-diphenyl-4,5-dihydro-1H-pyrazolo[4,3-e][1,2,4]triazolo[4,3-a]pyrimidin-8-yl)sulfanylacetate (12)

Method A

A mixture of the thioxo derivative **10** (0.36 g, 1 mmol), ethyl bromoacetate (0.2 g, 0.13 ml, 1.2 mmol) and anhydrous potassium carbonate (0.17 g, 1.2 mmol) in dry dimethylformamide (5 ml) was stirred at room temperature for 24 h, then the reaction mixture was poured into ice-cold water, the separated solid was filtered, washed with water, dried and crystallized from dioxane. Yield 64%, Mp. > 300 °C.

Method B

A mixture of the selected aryl thiosemicarbazide **9a-d** (1 mmol) and ethyl bromoacetate (0.2 g, 0.13 ml, 1.2 mmol) in absolute ethanol (10 ml) was heated under reflux for 8 h. The separated white solid was filtered while hot, washed with ethanol, dried and recrystallized from dioxane. Yield 77%, Mp. > 300 °C.

IR (KBr, cm^{-1}): 3054, 2989, 2944 (CH); 1734, 1710 (C═O); 1610 (C═N); 1558, 1503 (C═C); 1310, 1128 (C—S—C); 1261, 1012 (C—O—C). ^{1}H NMR (300 MHz, DMSO-d_6) δ 1.24 (t, J = 7.2 Hz, 3H, $CH_2\underline{CH_3}$); 4.49 (q, J = 7.2 Hz, 2H, $\underline{CH_2}CH_3$); 4.27 (s, 2H, CH_2); 7.29–7.73 (m, 8H, phenyl-H); 8.00 (dd, J = 7.8, 1.2 Hz, 2H, phenyl $C_{2,6}$-H); 8.41 (s, 1H, pyrazolotriazolopyrimidinone C_3-H). ^{13}C NMR spectrum (75 MHz, DMSO-d_6) δ 14.52 (CH_3); 39.66 (S-CH_2); 62.28 (OCH_2); 103.24 (pyrazolotriazolopyrimidinone C_{3a}); 121.31, 127.03, 127.79, 129.63, 130.48, 131.11, 131.47, 137.14, 138.99 (two phenyl-C and pyrazolotriazolopyrimidinone C_3); 150.49, 150.95, 151.94, 152.46 (pyrazolotriazolopyrimidinone $C_{4,5a,8,9a}$); 167.98 (ester C═O). Anal. Calcd for $C_{22}H_{18}N_6O_3S$ (446.48): C, 59.18; H, 4.06; N, 18.82; S, 7.18 Found: C, 59.37; H, 4.15; N, 19.04; S, 7.29.

4.2. Biological evaluation

4.2.1. In vitro cyclooxygenase inhibition assay

The ability of the tested compounds to inhibit both COX-1 and COX-2 isozymes at three concentrations (25, 50 and 100 μM) was carried out as reported earlier [9].

4.2.2. In vivo anti-inflammatory activity

Adult Female Wistar rats weighing 150–250 g were used (procured from the Experimental Animal Centre in Alexandria University). All animals accessed to food and water *ad libitum* and were housed in 12 h dark/light cycle in a controlled condition at 23–25 °C. They were allowed to acclimatize for 1 week prior to experimentation. Procedures involving animals and their care were conducted in conformity with the Guide for the Care and Use of Laboratory Animals published by US

National Institute of Health (NIH publication No. 83-23, revised 1996) and following the ethical guidelines of Alexandria University on laboratory animals. In all tests, adequate considerations were adopted to reduce pain or discomfort of animals.

Compounds that showed *in vitro* selectivity indices higher or nearly equivalent to reference drugs towards COX-2 enzyme **(2c, 2d, 3e, 3g, 3i, 4a, 6a, 8** and **12)** were further evaluated for their *in vivo* anti-inflammatory activity applying the formalin-induced paw edema screening protocol as an acute inflammation model [38,39] and cotton pellet-induced granuloma protocol as a chronic inflammation model [40]. All procedures for both protocols were conducted as reported earlier [9].

4.2.3. Ulcerogenic activity

The selected compounds were also evaluated for chronic gastric ulcerogenic effect [41,42] on the same groups of rats. All procedures were conducted as reported earlier [9].

4.3. Molecular modeling

4.3.1. Molecular docking

Preparation of target proteins

The coordinates of the X-ray crystal structure of COX-1 (PDB ID: 1EQG) and COX-2 (PDB ID: 5IKQ) were obtained from Protein Data Bank and used directly from previous study. [26]

Preparation of the selected compounds for docking

The compounds were built and prepared by Molecular Operating Environment (MOE) [12]. Generation of meaningful protonation states, energy minimization steps and calculation of partial charges were conducted as reported earlier [26]. The prepared molecules were then saved as SD file for the docking runs.

Docking experiments

GOLD (version 5.2) [50–53] was used for employing the scoring functions ChemPLP for the docking experiments against COX-1 and COX-2 models. The definition of the binding site and search efficiency were conducted as reported earlier [26]. All graphical representations in Figs. 3–7 were rendered by MOE.

4.3.2. Assessment of drug likeness score, toxicities profiles as well as in silico prediction of physicochemical properties and pharmacokinetic profile

The biologically active compounds **(2c, 2d, 3e, 3g, 3i, 4a, 6a, 8** and **12)** were subjected to physical and molecular prediction tools, namely: PreADMET [54], Molinspiration [55], Molsoft [56] and Osiris [57] software packages.

Conflict of interest

The authors have declared no conflict of interest.

Acknowledgments

The authors wish to express their thanks to Dr.Waleed Ali Mohamed, Assistant professor of Medicinal Biochemistry, Faculty of Medicine, Cairo University, for carrying out the *in vitro* anti-inflammatory screening. TMI acknowledges Prof. Dr. Frank Boeckler, Lab for Molecular Design & Pharmaceutical Biophysics, Eberhard Karls University Tuebingen, Germany, for granting access to some computational tools.

Appendix A. Supplementary material

Supplementary data to this article can be found online at https://doi.org/10.1016/j.bioorg.2019.03.018.

References

[1] S. Fiorucci, R. Meli, M. Bucci, G. Cirino, Dual inhibitors of cyclooxygenase and 5-lipoxygenase. A new avenue in anti-inflammatory therapy? Biochem. Pharmacol. 62 (2001) 1433–1438.
[2] S. Bacchi, P. Palumbo, A. Sponta, M. Coppolino, Clinical pharmacology of non-steroidal anti-inflammatory drugs: a review, Antiinflamm. Antiallergy Agents Med. Chem. 11 (2012) 52–64.
[3] B.J. Whittle, Mechanisms underlying intestinal injury induced by anti-inflammatory COX inhibitors, Eur. J. Pharmcol. 500 (2004) 427–439.
[4] M. Abdel-Tawab, H. Zettl, M. Schubert-Zsilavecz, Nonsteroidal anti-inflammatory drugs: a critical review on current concepts applied to reduce gastrointestinal toxicity, Curr. Med. Chem. 16 (2009) 2042–2063.
[5] A. Bruno, S. Tacconelli, P. Patrignani, Variability in the response to non-steroidal anti-inflammatory drugs: mechanisms and perspectives, Basic Clin. Pharmacol. Toxicol. 114 (2014) 56–63.
[6] M.M. Goldenberg, Celecoxib, a selective cyclooxygenase-2 inhibitor for the treatment of rheumatoid arthritis and osteoarthritis, Clin. Therapeut. 21 (1999) 1497–1513.
[7] S.D. Solomon, J. Wittes, P.V. Finn, R. Fowler, J. Viner, M.M. Bertagnolli, N. Arber, B. Levin, C.L. Meinert, B. Martin, Cardiovascular risk of celecoxib in 6 randomized placebo-controlled trials the cross trial safety analysis, Circulation 117 (2008) 2104–2113.
[8] G.N. Tageldin, S.M. Fahmy, H.M. Ashour, M.A. Khalil, R.A. Nassra, I.M. Labouta, Design, synthesis and evaluation of some pyrazolo[3,4-d]pyrimidine derivatives bearing thiazolidinone moiety as anti-inflammatory agents, Bioorg. Chem. 80 (2018) 164–173.
[9] G.N. Tageldin, S.M. Fahmy, H.M. Ashour, M.A. Khalil, R.A. Nassra, I.M. Labouta, Design, synthesis and evaluation of some pyrazolo[3,4-d]pyrimidines as anti-inflammatory agents, Bioorg. Chem. 78 (2018) 358–371.
[10] H.A. Abd El Razik, M. Mroueh, W.H. Faour, W.N. Shebaby, C.F. Daher, H. Ashour, H.M. Ragab, Synthesis of new pyrazolo [3, 4-d] pyrimidine derivatives and evaluation of their anti-inflammatory and anticancer activities, Chem. Biol. Drug Des. 90 (2017) 83–96.
[11] K.R.A. Abdellatif, R.B. Bakr, New advances in synthesis and clinical aspects of pyrazolo[3,4-d]pyrimidine scaffolds, Bioorg. Chem. 78 (2018) 341–357.
[12] S. Alcaro, A. Artese, M. Botta, A.T. Zizzari, F. Orallo, F. Ortuso, S. Schenone, C. Brullo, M. Yáñez, Hit identification and biological evaluation of anticancer pyrazolopyrimidines endowed with anti-inflammatory activity, ChemMedChem 5 (2010) 1242–1246.
[13] S.B. Yewale, S.B. Ganorkar, K.G. Baheti, R.U. Shelke, Novel 3-substituted-1-aryl-5-phenyl-6-anilinopyrazolo [3, 4-d] pyrimidin-4-ones: Docking, synthesis and pharmacological evaluation as a potential anti-inflammatory agents, Bioorg. Med. Chem. Lett. 22 (2012) 6616–6620.
[14] H.H. Kadry, Synthesis, biological evaluation of certain pyrazolo[3,4-d]pyrimidines as novel anti-inflammatory and analgesic agents, Med. Chem. Res. 23 (2014) 5269–5281.
[15] J.M. Quintela, C. Peinador, L. González, I. Devesa, M.L. Ferrándiz, M.J. Alcaraz, R. Riguera, 6-Dimethylamino 1H-pyrazolo [3, 4-d] pyrimidine derivatives as new inhibitors of inflammatory mediators in intact cells, Bioorg. Med. Chem. 11 (2003) 863–868.
[16] I. Devesa, M.J. Alcaraz, R. Riguera, M.L. Ferrándiz, A new pyrazolo pyrimidine derivative inhibitor of cyclooxygenase-2 with anti-angiogenic activity, Eur. J. Pharmcol. 488 (2004) 225–230.
[17] R.S. Sinatra, J.S. Jahr, J.M. Watkins-Pitchford, The Essence of Analgesia and Analgesics, Cambridge University Press, 2010.
[18] A.H. Abdelazeem, S.A. Abdelatef, M.T. El-Saadi, H.A. Omar, S.I. Khan, C.R. McCurdy, S.M. El-Moghazy, Novel pyrazolopyrimidine derivatives targeting COXs and iNOS enzymes; design, synthesis and biological evaluation as potential anti-inflammatory agents, Eur. J. Pharm. Sci. 62 (2014) 197–211.
[19] H. Kumar, S.A. Javed, S.A. Khan, M. Amir, 1, 3, 4-Oxadiazole/thiadiazole and 1, 2, 4-triazole derivatives of biphenyl-4-yloxy acetic acid: Synthesis and preliminary evaluation of biological properties, Eur. J. Med. Chem. 43 (2008) 2688–2698.
[20] S.M. El-Moghazy, F.F. Barsoum, H.M. Abdel-Rahman, A.A. Marzouk, Synthesis and anti-inflammatory activity of some pyrazole derivatives, Med. Chem. Res. 21 (2012) 1722–1733.
[21] E.S. Al-Abdullah, H.H. Asiri, S. Lahsasni, E.E. Habib, T.M. Ibrahim, A.A. El-Emam, Synthesis, antimicrobial, and anti-inflammatory activity, of novel S-substituted and N-substituted 5-(1-adamantyl)-1, 2, 4-triazole-3-thiols, Drug Des. Devel. Ther. 8 (2014) 505.
[22] M. El Shehry, A. Abu-Hashem, E. El-Telbani, Synthesis of 3-((2, 4-dichlorophenoxy) methyl)-1, 2, 4-triazolo (thiadiazoles and thiadiazines) as anti-inflammatory and molluscicidal agents, Eur. J. Med. Chem. 45 (2010) 1906–1911.
[23] O.H. Rizk, O.G. Shaaban, I.M. El-Ashmawy, Design, synthesis and biological evaluation of some novel thienopyrimidines and fused thienopyrimidines as anti-inflammatory agents, Eur. J. Med. Chem. 55 (2012) 85–93.
[24] M. Khoshneviszadeh, M.H. Ghahremani, A. Foroumadi, R. Miri, O. Firuzi, A. Madadkar-Sobhani, N. Edraki, M. Parsa, A. Shafiee, Design, synthesis and biological evaluation of novel anti-cytokine 1, 2, 4-triazine derivatives, Bioorg. Med. Chem. 21 (2013) 6708–6717.
[25] C.M. Bhalgat, M.I. Ali, B. Ramesh, G. Ramu, Novel pyrimidine and its triazole fused derivatives: synthesis and investigation of antioxidant and anti-inflammatory activity, Arab. J. Chem. 7 (2014) 986–993.
[26] A.A. Bekhit, A.M. Farghaly, R.M. Shafik, M.M. Elsemary, M.S. El-Shoukrofy, A.E.-D.A. Bekhit, T.M. Ibrahim, Synthesis, evaluation and modeling of some

triazolothienopyrimidinones as anti-inflammatory and antimicrobial agents, Future Med. Chem. 9 (2017) 881–897.
[27] H.M. Ashour, O.G. Shaaban, O.H. Rizk, I.M. El-Ashmawy, Synthesis and biological evaluation of thieno [2′, 3′: 4, 5] pyrimido [1, 2-b][1, 2, 4] triazines and thieno [2, 3-d][1, 2, 4] triazolo [1, 5-a] pyrimidines as anti-inflammatory and analgesic agents, Eur. J. Med. Chem. 62 (2013) 341–351.
[28] M. El-Kerdawy, M. El-Ashmawy, I. Shehata, A. Eldin, A. Barghash, E. El-Bendary, H. El-Khashef, Fused pyrimidines: synthesis and anti-inflammatory testing of certain novel imidazo [1, 2-c] quinazoline, pyrazolo [3, 4-d] triazolo [3, 4-b] pyrimidine and pyrimido [2, 1-a] phthalazine derivatives, Saudi. Pharm. J. 5 (1997) 46–51.
[29] M. Shaaban, A. Abou Sier, A. El-Ansary, H. Kadry, H. Abd El-Latif, Synthesis and pharmacological activities of certain pyrazolotriazolopyrimidine and pyrazolotriazepine derivatives, Bull. Fac. Pharm. Cairo. Univ. 39 (2001) 67–77.
[30] F. Russo, S. Guccione, G. Romeo, L. Monsu'Scolaro, S. Pucci, A. Caruso, V. Cutuli, M.A. Roxas, Synthesis and pharmacological properties of pyrazolotriazolopyrimidine derivatives, Eur. J. Med. Chem. 27 (1992) 73–80.
[31] T.M. Ibrahim, M.R. Bauer, A. Dorr, E. Veyisoglu, F.M. Boeckler, pROC-Chemotype plots enhance the interpretability of benchmarking results in structure-based virtual screening, J. Chem. Inf. Model. 55 (2015) 2297–2307.
[32] A. Malki, H.M. Ashour, R.Y. Elbayaa, D.A. Issa, H.A. Aziz, X. Chen, Novel 1, 5-diphenyl-6-substituted 1H-pyrazolo [3, 4-d] pyrimidin-4 (5 H)-ones induced apoptosis in RKO colon cancer cells, J. Enzyme Inhib. Med. Chem. 1–14 (2015).
[33] S.A. Hasan, A.N. Elias, Synthesis of new Diclofenac derivatives by coupling with chalcone derivatives as possible mutual prodrugs, Int. J. Pharm. Pharm. Sci. 6 (2014) 239–245.
[34] S.V. Bhandari, K.G. Bothara, M.K. Raut, A.A. Patil, A.P. Sarkate, V.J. Mokale, Design, synthesis and evaluation of antiinflammatory, analgesic and ulcerogenicity studies of novel S-substituted phenacyl-1,3,4-oxadiazole-2-thiol and Schiff bases of diclofenac acid as nonulcerogenic derivatives, Bioorg. Med. Chem. 16 (2008) 1822–1831.
[35] M. Kira, M. Abdel-Rahman, K. Gadalla, The Vilsmeier-Haack reaction-III cyclization of hydrazones to pyrazoles, Tetrahedron Lett. 10 (1969) 109–110.
[36] V. Chenna, C. Hu, S.R. Khan, Synthesis and cytotoxicity studies of Hedgehog enzyme inhibitors SANT-1 and GANT-61 as anticancer agents, J. Environ. Sci. Health A 49 (2014) 641–647.
[37] C.-J. Xu, Y.-Q. Shi, Synthesis and crystal structure of 5-chloro-3-methyl-1-phenyl-1H-pyrazole-4-carbaldehyde, J. Chem. Crystal. 41 (2011) 1816–1819.
[38] P. Subramanium, Evaluation of anti-inflammatory and analgesic activities of methanolic leaf extract of the endangered tree species, Hildegardia populifolia (Roxb.) Schott and Endl, Int. J. Green Pharm. 9 (2015) 125–130.
[39] A. Razmi, A. Zarghi, S. Arfaee, N. Naderi, M. Faizi, Evaluation of anti-nociceptive and anti-inflammatory activities of novel chalcone derivatives, Iran. J. Pharm. Res. 12 (2013) 153–159.
[40] N. Mishra, R. Panda, G. Mishra, V. Rajakumar, S. Kumar, K. Tejonidhi, Screening of anti-inflammatory activity and dose selection of Mollugo pentaphylla by using cotton pellet induced, Int. J. Pharmacy Life Sci. 2 (2011).
[41] S. Srivastava, C. Nath, M. Gupta, S. Vrat, J. Sinha, K. Dhawan, G. Gupta, Protection against gastric ulcer by verapamil, Pharmacol. Res. 23 (1991) 81–86.
[42] V. Lakshmi, V. Mishra, G. Palit, A new gastroprotective effect of limonoid compounds xyloccensins x and y from xylocarpus molluccensis in rats, Nat. Prod. Bioprospect. 4 (2014) 277–283.
[43] C. Charlier, C. Michaux, Dual inhibition of cyclooxygenase-2 (COX-2) and 5-lipoxygenase (5-LOX) as a new strategy to provide safer non-steroidal anti-inflammatory drugs, Eur. J. Med. Chem. 38 (2003) 645–659.
[44] G. Dannhardt, W. Kiefer, Cyclooxygenase inhibitors–current status and future prospects, Eur. J. Med. Chem. 36 (2001) 109–126.
[45] R.G. Kurumbail, A.M. Stevens, J.K. Gierse, J.J. McDonald, R.A. Stegeman, J.Y. Pak, D. Gildehaus, J.M. Miyashiro, T.D. Penning, K. Seibert, P.C. Isakson, W.C. Stallings, Structural basis for selective inhibition of cyclooxygenase-2 by anti-inflammatory agents, Nature 384 (1996) 644–648.
[46] M.R. Bauer, T.M. Ibrahim, S.M. Vogel, F.M. Boeckler, Evaluation and optimization of virtual screening workflows with DEKOIS 2.0–a public library of challenging docking benchmark sets, J. Chem. Inf. Model. 53 (2013) 1447–1462.
[47] T.M. Ibrahim, M.R. Bauer, F.M. Boeckler, Applying DEKOIS 2.0 in structure-based virtual screening to probe the impact of preparation procedures and score normalization, J. Cheminform., 7 (2015) 21.
[48] F.M. Boeckler, M.R. Bauer, T.M. Ibrahim, S.M. Vogel, Use of DEKOIS 2.0 to gain insights for virtual screening, J. Cheminform. 6 (2014) O24.
[49] A.A. Bekhit, A.M. Farghaly, R.M. Shafik, M.M.A. Elsemary, A.E.A. Bekhit, A.A. Guemei, M.S. El-Shoukrofy, T.M. Ibrahim, Synthesis, biological evaluation and molecular modeling of novel thienopyrimidinone and triazolothienopyrimidinone derivatives as dual anti-inflammatory antimicrobial agents, Bioorg. Chem. 77 (2018) 38–46.
[50] M.J. Hartshorn, M.L. Verdonk, G. Chessari, S.C. Brewerton, W.T. Mooij, P.N. Mortenson, C.W. Murray, Diverse, high-quality test set for the validation of protein-ligand docking performance, J. Med. Chem. 50 (2007) 726–741.
[51] G. Jones, P. Willett, R.C. Glen, Molecular recognition of receptor sites using a genetic algorithm with a description of desolvation, J. Mol. Biol. 245 (1995) 43–53.
[52] G. Jones, P. Willett, R.C. Glen, A genetic algorithm for flexible molecular overlay and pharmacophore elucidation, J. Comput.-Aided Mol. Des. 9 (1995) 532–549.
[53] G. Jones, P. Willett, R.C. Glen, A.R. Leach, R. Taylor, Development and validation of a genetic algorithm for flexible docking, J. Mol. Biol. 267 (1997) 727–748.
[54] < https://preadmet.bmdrc.kr/adme/ > .
[55] < http://www.molinspiration.com/cgi-bin/properties > .
[56] < http://molsoft.com/mprop/ > .
[57] < http://www.rdchemicals.com/drug-relevant-properties.html > .